

Dynamical formation & scattering of hierarchical triples: Cross sections, Kozai-Lidov oscillations, and collisions

Joseph M. O. Antognini^{1,2} and Todd A. Thompson^{1,2}

¹ *Department of Astronomy, The Ohio State University, Columbus, Ohio 43210, USA*

² *Center for Cosmology and Astro-Particle Physics, The Ohio State University, Columbus, Ohio 43210, USA*

E-mail: antognini@astronomy.ohio-state.edu

17 July 2018

ABSTRACT

Dynamical scattering of binaries and triple systems of stars, planets, and compact objects may produce highly inclined triple systems subject to Kozai-Lidov (KL) oscillations, potentially leading to collisions, mergers, Type Ia supernovae, and other phenomena. We present the results of more than 400 million gravitational scattering experiments of binary-binary, triple-single, and triple-binary scattering. We compute the cross sections for all possible outcomes and explore their dependencies on incoming velocity, mass, semi-major axis, and eccentricity, including analytic fits and discussion of the velocity dependence. For the production of new triple systems by scattering we find that compact triples are preferred, with ratios of outer to inner semi-major axes of \sim few–100, flat or quasi-thermal eccentricity distributions, and flat distributions in cosine of the mutual inclination. Dynamically formed triples are thus subject to strong KL oscillations, the “eccentric Kozai mechanism,” and non-secular effects. For single and binary flyby encounters with triple systems, we compute the cumulative cross section for changes to the mutual inclination, eccentricity, and semi-major axis ratio. We apply these results to scattering events in the field, open clusters, and globular clusters, and explore the implications for Type Ia supernovae via collisions and mergers, stellar collisions, and the lifetime and dynamical isolation of triple systems undergoing KL oscillations. An Appendix provides an analysis of the velocity dependence of the collision cross section in binary-single scattering.

1 INTRODUCTION

Gravitational scattering events are common in globular clusters and are also dynamically important for many systems in open clusters and the field (Hills & Day 1976). Although two-body scattering can be studied analytically, three-body scattering is too complex to permit general, practical analytic results (Poincaré 1892; Sundman 1907). The three-body scattering problem was therefore not studied in detail until the development of computers (e.g., Saslaw et al. 1974; Heggie 1975; Hut & Bahcall 1983). Since then binary-single and binary-binary scattering events have been studied extensively (e.g., Hut 1983; Mikkola 1983; Hills 1991; Valtonen & Mikkola 1991; Sigurdsson & Phinney 1993; Bacon et al. 1996; Fregeau et al. 2004, and the references therein), but little attention has been devoted to the scattering of triple systems or to the orbital characteristics of triple systems formed from binary-binary scattering (though see Ivanova 2008; Ivanova et al. 2008; Leigh et al. 2011; Leigh & Geller 2012; Moeckel & Bonnell 2013; Leigh & Geller 2013, 2015). Yet due to the Kozai-Lidov (KL) mechanism (Lidov 1962; Kozai 1962), it is now appreciated that the dynamics of triples may play an important role in a wide vari-

ety of astrophysical phenomena (e.g., Holman et al. 1997; Ford et al. 2000; Miller & Hamilton 2002; Blaes et al. 2002; Wu & Murray 2003; Wen 2003; Fabrycky & Tremaine 2007; Wu et al. 2007; Ivanova et al. 2008; Perets & Fabrycky 2009; Naoz et al. 2011; Thompson 2011; Naoz et al. 2012; Katz & Dong 2012; Shappee & Thompson 2013; Antonini et al. 2014; Antognini et al. 2014). Furthermore, it is now known that triple systems are not rare in our Galaxy; demographic surveys of the field have revealed that triples constitute 10% of all stellar systems (Duquennoy & Mayor 1991; Raghavan et al. 2010; Tokovinin 2014; Sana et al. 2014).

Given the prevalence of triple systems it is important to understand in detail how triples interact with other stellar systems. Observations of the Tarantula Nebula have demonstrated that binary interactions strongly affect the observed multiplicity fraction (Sana et al. 2013) so triple interactions may contribute to the observed multiplicity fraction as well. Moreover, the large multiplicity fraction of high mass stars indicates that triple dynamics may be even more important for these systems (Leigh & Geller 2013); for example, scattering of triples with binaries may be an important formation mechanism for quadruple systems. Raghavan et al.

(2010) showed that quadruple systems are nearly as common as triple systems and many even higher-order systems have been discovered (e.g., Koo et al. 2014), but it is unclear what fraction of such systems are formed *in situ* versus dynamically (Goodwin & Kroupa 2005). Quadruple and higher-order systems may be even more dynamically important than triples since numerical and semi-analytic experiments have demonstrated that they exhibit stronger KL oscillations than triples over a wider region of parameter space (Pejcha et al. 2013; Hamers et al. 2015).

The perturbative influence of interloping stars on hierarchical triple systems may have an important effect on the long-term evolution of triples. The KL mechanism can drive the inner binary to very high eccentricities, but the maximum eccentricity reached is sensitive to the orbital parameters, in particular the mutual inclination and the outer eccentricity. In the standard quadrupole order KL mechanism the tertiary can drive the inner binary to arbitrarily large eccentricities over a narrow range of inclinations near 90° (the exact value depends on the particular system). However, at octupole order, in the so-called “eccentric KL mechanism,” the range of inclinations over which the tertiary can drive the inner binary to extreme eccentricities is significantly increased, especially if the eccentricity of the orbit of the tertiary is large. Thus, perturbations to the inclination or eccentricity of the tertiary may produce much stronger KL oscillations for star-star or star-planet systems. If these KL oscillations drive the inner binary to sufficiently high eccentricities, the components of the inner binary will tidally interact (e.g., Mazeh & Shaham 1979; Wu & Murray 2003; Fabrycky & Tremaine 2007; Perets & Fabrycky 2009; Naoz et al. 2011, 2012; Naoz & Fabrycky 2014), potentially explaining the observation that nearly all close binaries (Tokovinin et al. 2006) and certain subsets of warm and hot Jupiters (Wu & Murray 2003; Wu et al. 2007; Naoz et al. 2011, 2012; Socrates et al. 2012; Dong et al. 2014) have tertiary companions.

Tidal interactions may not always occur in highly inclined triple systems; Li et al. (2014) showed that some coplanar systems can be driven to very large eccentricities. Moreover, certain systems undergo changes in eccentricity so rapidly that the angular momentum of the inner orbit can change by an order of magnitude in a single orbit (Antonini & Perets 2012; Katz & Dong 2012; Seto 2013; Antonini et al. 2014; Antognini et al. 2014). These rapid eccentricity oscillations present the possibility that the components of the inner orbit may be driven to merger more rapidly than the tidal circularization process can circularize the orbit and quench KL oscillations. The components of the inner binaries of such systems will then not merge gently, but will instead collide head-on. These head-on collisions may produce a variety of unusual astrophysical phenomena depending on the objects comprising the inner binary. Most notably, if the inner binary components are two white dwarfs, these collisions may produce a Type Ia supernova (SN Ia; Thompson 2011; Katz & Dong 2012; Hamers et al. 2013; Kushnir et al. 2013; Prodan et al. 2013).

The possible connection between triple dynamics and SNe Ia should be explored because, despite their crucial role in constraining cosmological parameters (Riess et al. 1998; Perlmutter et al. 1999), it is unknown whether the progenitor systems consist of one white dwarf (the single degener-

ate model; Whelan & Iben 1973; Nomoto 1982) or two (the double degenerate model; Iben & Tutukov 1984; Webbink 1984). Although observational evidence currently favors the double degenerate model (Howell 2011; Maoz & Mannucci 2012; Maoz et al. 2014), it is unclear how to drive white dwarf binaries to merge at a rate large enough to be consistent with the observed SN Ia rate (Ruiter et al. 2009, 2011). One approach is by driving the binary to high eccentricity through the perturbative influence of a tertiary via the KL mechanism. At high eccentricities the inner binary would then emit much more gravitational radiation (Blaes et al. 2002; Miller & Hamilton 2002; Wen 2003), thereby leading to more rapid coalescence of the WD-WD binary (Thompson 2011). However, it is unclear how to prevent the inner binary from merging or colliding while still on the main sequence. KL oscillations would bring the two stars into tidal contact and tidal circularization would then shrink the orbit, greatly increasing the semi-major axis ratio and “freezing” the inner binary at an inclination close to the critical Kozai angle (Fabrycky & Tremaine 2007). These two effects would effectively shut off further KL oscillations and prevent the inner binary from merging when the stars evolve into white dwarfs. The dynamical formation of high-inclination triples from scattering may be one means to circumvent this difficulty.

Scattering of high-multiplicity systems may also be one channel to produce free-floating planets. Microlensing studies have revealed that there may be as many as two free-floating planets for every bound planet in the Galaxy (Zapatero Osorio et al. 2000; Sumi et al. 2011). Moreover, there is some evidence that it is difficult for planet-planet scattering to produce free floating planets in the required numbers (Veras & Raymond 2012). Dynamical scattering of field stars off of binary stars may be an important component to the rate of planet ejection.

Scattering events involving high-order stellar systems could also be a source of stellar collisions. Stellar collisions are estimated to occur at a rate of $\sim 0.5 \text{ yr}^{-1}$ in the Galaxy (Kochanek et al. 2014) and it is unknown whether these collisions are due to KL oscillations, scattering events, or a combination of the two. Even when scattering does not lead to a stellar collision the scattering event will change the orbital parameters of the system. This will lead to evolution in the distribution of orbital parameters of the triples in the population. This evolution would be strongest in globular clusters due to their high stellar densities and large ages.

This paper has three goals. The first is to perform idealized binary-binary, triple-single, and triple-binary scattering experiments in order to derive general relationships between the cross sections of various outcomes with the initial orbital parameters and the incoming velocity. In this way our paper is similar to Hut & Bahcall (1983) and Mikkola (1983) except that we study higher-order scattering. The second goal of our paper is to determine the orbital parameters of triple systems after scattering events. The final goal of our paper is to apply the cross sections we derive in several contexts. In particular we estimate the rate of formation of WD-WD binaries in highly inclined triples, the ejection rate of planets due to scattering events, the stellar collision rate, and the lifetime of high inclination triples. To meet these goals we have performed over 400 million scattering experiments.

Details of the numerical methods of this paper are pre-

sented in Section 2. We study triple scattering in detail in Section 3 by performing numerical experiments and comparing them with analytic approximations in Section 4. We then discuss the distribution of orbital parameters of dynamically formed triples in Section 5. We discuss the implications of these results for SNe Ia, the longevity of triple systems undergoing KL oscillations, and provide estimates for the rate of planetary ejection and stellar collisions in Section 6. We conclude in Section 7.

2 NUMERICAL METHODS

We use the open source FEWBODY suite to perform our scattering experiments (Fregeau et al. 2004). FEWBODY is optimized to numerically compute the dynamics of systems with small numbers of components ($N \lesssim 10$). FEWBODY uses the ordinary differential equations library of the GNU Scientific Library (GSL) for its underlying integrator (Gough 2009). The GSL ordinary differential equations library supports six integration algorithms with adaptive time steps, from which we use eighth-order Runge-Kutta Prince-Dormand integration. We find, however, that the choice of integration algorithm makes little difference to the results of the calculations because GSL’s adaptive time steps are chosen to target a specified relative and absolute accuracy (10^{-14} in our experiments) regardless of the algorithm used. FEWBODY also supports the use of Kustaanheimo-Stiefel (KS) regularization (Kustaanheimo & Stiefel 1965), a coordinate transformation which removes the singularities in the gravitational force present in ordinary N -body integration. Throughout this paper we use KS regularization as it has the particular advantage of making eccentric orbits much easier to compute.

2.1 Notation

Throughout this paper we use the same notation as Fregeau et al. (2004) and FEWBODY in which each star in a system with n stars is labelled with a unique index running from 0 to $n - 1$. Bound pairs are denoted by square brackets surrounding the pair and collisions between two stars are denoted by colons between the pair. For example, a hierarchical triple with an unbound interloping star is notated $[[0\ 1]\ 2]\ 3$ (stars 0 and 1 form the inner binary, star 2 is the tertiary, and star 3 is the interloping star), and a hierarchical triple in which the two stars of the inner binary have collided is notated $[0:1\ 2]$.

Orbital parameters (e.g., semi-major axis or eccentricity) of the component binaries of the system are notated by subscripts in a top-down fashion. Leftmost indices in subscripts represent the outermost binaries of the separate hierarchies, and rightward indices represent inner binaries in those hierarchies. For example, in a triple-binary scattering event, the semi-major axis of the outer binary of the triple is a_1 , the semi-major axis of the inner binary of the triple is a_{11} , and the semi-major axis of the interloping binary is a_2 . Similarly, the mass of the second star in the innermost binary of the triple is m_{112} , the mass of the tertiary is m_{12} , and the mass of the first star of the interloping binary is m_{21} . We also combine masses in the subscripts. Thus the total

mass in the inner binary of the triple is $m_{11} = m_{111} + m_{112}$ and the total mass of the triple is $m_1 = m_{11} + m_{12}$.

For clarity we occasionally refer to the orbital parameters of hierarchical triples using the subscripts “in” and “out.” Thus the eccentricity of the inner orbit of a triple may be referred to equivalently by e_{11} or e_{in} and the eccentricity of the outer orbit by e_1 or e_{out} .

2.2 Cross sections

Throughout this paper we provide cross sections for the outcomes of scattering events involving triple or higher-order hierarchical systems. Our treatment of these cross sections and their uncertainties follows that of Hut & Bahcall (1983). We use the usual definition of the cross section for a particular outcome, X :

$$\sigma_X = \pi b_{\max}^2 \frac{n_X}{n_{\text{tot}}}, \quad (1)$$

where b_{\max} is the maximum impact parameter in a set of experiments, n_X is the number of experiments with outcome X , and n_{tot} is the total number of experiments performed. Throughout this paper we present our results using normalized cross sections, $\hat{\sigma}$. The cross sections from triple-single scattering experiments are normalized to the area of the outer binary of the triple:

$$\hat{\sigma} \equiv \frac{\sigma}{\pi a_1^2} \quad (\text{triple-single}). \quad (2)$$

The cross sections for binary-binary experiments are normalized to the sum of the areas of the two binaries and similarly in triple-binary experiments the cross sections are normalized to the sum of the areas of the outer binary of the triple and the interloping binary:

$$\hat{\sigma} \equiv \frac{\sigma}{\pi(a_1^2 + a_2^2)} \quad (\text{binary-binary, triple-binary}). \quad (3)$$

There are two uncertainties in the calculation of the cross sections. The first is the statistical uncertainty due to the finite number of experiments performed:¹

$$\Delta_{\text{stat}} \sigma_X = \frac{\sigma_X}{\sqrt{n_X}}. \quad (4)$$

The second source of uncertainty is due to the fact that certain systems require prohibitively long computation times to resolve. For example, while it is impossible for a single star scattering off of a triple system to produce a stable quadruple system (Chazy 1929; Littlewood 1952; Heggie 1975; Heggie & Hut 2003), certain systems can enter into a “metastable” state where a quadruple system is produced that takes an exceedingly long time to dissociate. Such unresolved systems produce a separate systematic uncertainty in the calculation of the cross sections given by

$$\Delta_{\text{sys}} \sigma_X = \pi b_{\max}^2 \frac{n_{\text{unres}}}{n_{\text{tot}}}, \quad (5)$$

¹ In cases where the fraction of outcomes with the outcome X is close to unity or zero it is better to use a confidence interval like the Wilson score interval rather than the normal approximation in order to capture the asymmetry of the statistical uncertainty (Wilson 1927). However, we perform enough experiments that the difference between the Wilson score interval and the normal approximation is almost always negligible. Where it is not, we use the Wilson score interval.

where n_{unres} is the number of experiments with unresolved outcomes.

It is important to note that the systematic uncertainty is completely asymmetric and only serves to increase the cross section of any outcome. That is to say, our estimates of the cross sections are lower bounds on the true cross sections.

2.3 Initial conditions and halting criteria

Each scattering experiment begins with the interloping system at a large, but finite, distance from the target system. We choose the initial separation between the two systems to be the distance at which the tidal force on the outer binary of the target system is some small fraction, δ , of the relative force between the two components of the outer binary when at apocenter. Hence, the initial separation, r , is given by

$$\frac{F_{\text{tid}}}{F_{\text{rel}}} = \delta, \quad (6)$$

where

$$F_{\text{tid}} = \frac{2G(m_{11} + m_{12})m_2}{r^3} a(1 + e), \quad (7)$$

and

$$F_{\text{rel}} = \frac{Gm_{11}m_{12}}{[a(1 + e)]^2}, \quad (8)$$

where a and e refer to the semi-major axis and eccentricity, respectively, of the outer binary of the target system. Throughout this paper we use $\delta = 10^{-5}$, the same choice as Fregeau et al. (2004). Smaller choices of δ do not change the results but increase the running time. The interloping system is then analytically brought along a hyperbolic orbit from infinity with the b_{max} and velocity at infinity, v_{∞} , that has been fixed for that particular experiment.

It is also essential to choose the appropriate b_{max} when computing cross sections. Too small a choice of b_{max} will result in an underestimate of the cross section, whereas too large a choice of b_{max} will result in few experiments producing outcomes of interest, thereby leading to large statistical uncertainties. We adopt the choice of b_{max} similar to that of Hut & Bahcall (1983) of:

$$b_{\text{max}} = \left(\frac{4v_{\text{crit}}}{v_{\text{inf}}} + 3 \right) a_1, \quad (9)$$

where v_{inf} is the incoming velocity at infinity and v_{crit} is the critical velocity at which the total energy of the system is zero. For binary-binary scattering, v_{crit} is

$$v_{\text{crit, bin-bin}}^2 = \frac{G(m_1 + m_2)}{m_1 m_2} \left(\frac{m_{11}m_{12}}{a_1} + \frac{m_{21}m_{22}}{a_2} \right), \quad (10)$$

for triple-single scattering, v_{crit} is

$$v_{\text{crit, trip-sing}}^2 = \frac{G(a_1 m_{111} m_{112} + a_{11} m_{11} m_{12})(m_1 + m_2)}{a_1 a_{11} m_1 m_2}, \quad (11)$$

and for triple-binary scattering v_{crit} is

$$v_{\text{crit, trip-bin}}^2 = \frac{G(m_1 + m_2)}{a_1 a_{11} a_2 m_1 m_2} \times [a_{11} a_2 m_{11} m_{12} + a_1 (a_2 m_{111} m_{112} + a_{11} m_{21} m_{22})]. \quad (12)$$

We will frequently refer to velocities in terms of the normalized velocity, \hat{v} , which is the velocity, v , scaled to v_{crit} ,

$$\hat{v} \equiv \frac{v}{v_{\text{crit}}}. \quad (13)$$

We test our choice of b_{max} by computing the cross sections for four categories of outcome in triple-single scattering over a broad range of b_{max} . We demonstrate that the cross sections are well converged in Fig. 1.

The calculation halts when one of four conditions is met: (1) if the system consists of some number of stable hierarchical systems as determined by the Mardling stability criterion (Mardling & Aarseth 2001):

$$\frac{a_1}{a_{11}}(1 - e_1) > 2.8 \left[\left(1 + \frac{m_{11}}{m_{12}} \right) \frac{1 + e_1}{\sqrt{1 - e_1}} \right]^{2/5} \left(1 - \frac{0.3}{\pi} i \right) \quad (14)$$

(where the mutual inclination, i , is in radians), and all the systems are far enough apart that the ratios between their tidal forces to their relative forces is less than δ ; (2) the system integrates for 10^6 times the initial orbital period of the outer binary of the target system; (3) the system integrates for one hour; or (4) the total energy or angular momentum of the system changes from its initial value by more than one part in 10^3 . If conditions (2) or (3) are met the outcome is classified as unresolved and included in our systematic uncertainty.²

3 SCATTERING EXPERIMENTS

Hierarchical triples can be formed through scattering in one of three ways: (1) binary-binary scattering, (2) scattering of triples, or (3) scattering of higher-order systems. Binary-binary scattering has been studied extensively, but only rarely have any studies addressed the formation of triple systems and, moreover, scattering of higher-order systems in general has received little attention at all. We study triple and binary scattering in detail in this section. We do not study the scattering of higher-order systems (e.g., triple-triple, quadruple-single) because such scattering events are rare in most environments (Leigh & Geller 2013).

We compute the cross sections for the outcomes of both single and binary stars scattering off of hierarchical triples along with binaries scattering off of binaries in the point mass limit using Newtonian gravity. The masses of all stars in the system are equal unless we explicitly vary the mass of one star of the inner binary of the triple. In an individual scattering event, the semi-major axis and eccentricity of all component binaries (both binaries of the triple and, in the case of triple-binary scattering, that of the interloping binary) in the system are fixed, but the argument of pericenter

² Portegies Zwart & Boekholt (2014) have argued that typical energy conservation standards in N -body studies are extremely conservative and that maintaining energy conservation to better than one part in 10 is sufficient to preserve the statistical properties of dynamical experiments. These results have been confirmed by Boekholt & Portegies Zwart (2015). Since very few of our experiments violate our energy conservation standard, this finding does not change our results, but does imply that we may have slightly overestimated our systematic uncertainties.

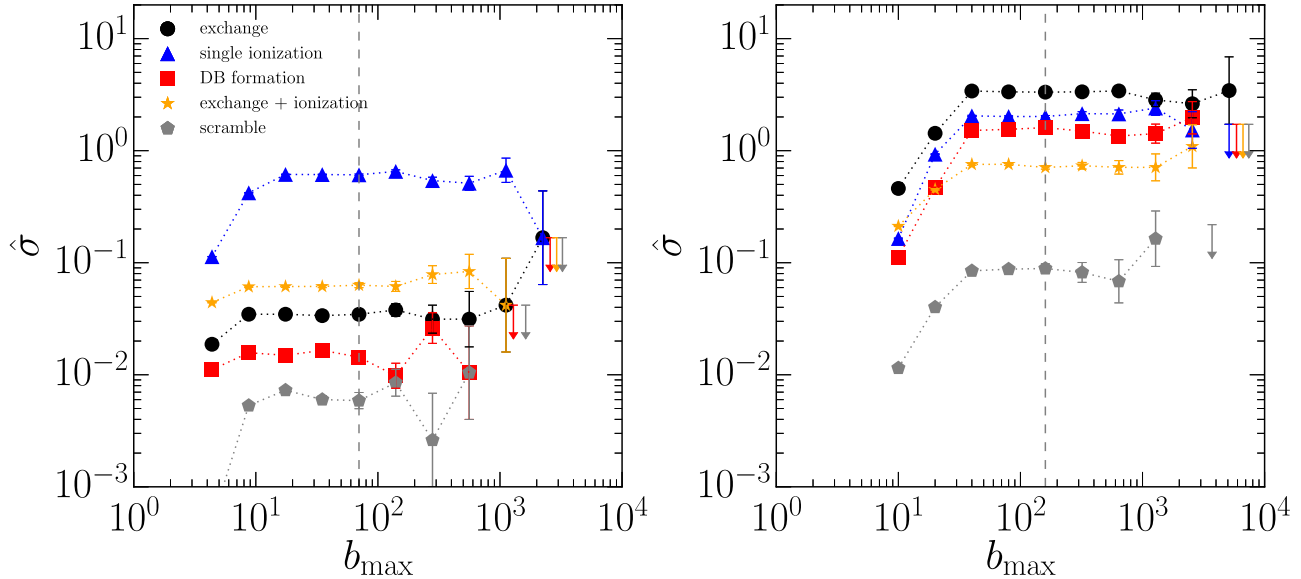


Figure 1. Convergence of the scattering cross sections with b_{\max} for triple-single scattering. We performed 3×10^5 scattering experiments at each choice of b_{\max} . *Left panel:* All masses are equal point masses and the orbits of the initial triple were circular with a semi-major axis ratio of 10. The cross sections for four categories of outcomes are presented: exchanges (black circles), single ionization (blue triangles), double binary formation (red squares), and exchange-ionization (orange stars). (See Section 3.2 for a description of the categories.) *Right panel:* Same as the left panel, but the mass of one star in the inner binary is set to be a test particle. The choice for b_{\max} we adopt in this paper (dashed line) is given by equation (9) and is similar to that of Hut & Bahcall (1983). Smaller b_{\max} 's do not probe the full area over which non-flyby outcomes occur, whereas the statistical power of larger b_{\max} 's is reduced because of the small fraction of non-flyby outcomes. The choice we adopt is converged but is small enough to have strong statistics.

and the mean anomaly are chosen from a uniform distribution between 0 and 2π . The component binaries are then oriented randomly by pointing each binary's angular momentum vector toward a randomly chosen point on a sphere. We present a sample binary-binary, triple-single, and triple-binary scattering experiment projected in the xy -plane in Fig. 2.

We first perform scattering experiments on a model system in Section 3.1 and then vary several of the initial orbital and physical parameters of this system one at a time to determine the dependence of the cross sections on these parameters in Section 3.2.

3.1 Cross sections of model systems

Our model system for triple-single scattering is a moderately hierarchical triple system with semi-major axis ratio, $\alpha \equiv a_1/a_{11} = 10$. This choice of α is large enough that the triple is stable (Mardling & Aarseth 2001), but is still small enough that there will be dynamical interactions between the inner and outer binaries. In this model system, the interloping star has an incoming velocity of $v_\infty/v_{\text{crit}} = 1$, which is approximately the velocity dispersion of stars in the thin disk of the Milky Way ($\sim 40 \text{ km s}^{-1}$) relative to the critical velocity of a triple system consisting of three $1 M_\odot$ stars with $a_1 = 10 \text{ AU}$ and $a_{11} = 1 \text{ AU}$ (Binney & Merrifield 1998, p. 656). We take both orbits to be circular.

Our model system for triple-binary scattering is identical, but with the interloping star replaced by an interloping binary with semi-major axis equal to the outer semi-major

axis of the triple, $a_2 = a_1 = 10a_{11}$. The incoming velocity is again taken to be v_{crit} , but with v_{crit} now calculated using equation (12) instead of equation (11). Again, all stars are of equal mass, so now the mass ratio of the interloping system to the triple is $2/5$ instead of $1/3$.

Lastly, our model system for binary-binary scattering is identical to the case of triple-binary scattering but with the inner binary of the triple replaced by a point mass of $1 M_\odot$. The incoming velocity is taken to be v_{crit} , but with v_{crit} calculated using equation (10). In this case the mass ratio of the interloping system to the target system is 1.

We perform 10^6 scattering experiments for each model system. We present the cross sections for all possible outcomes with their statistical and total uncertainties in Table 1 for the triple-single case, Table 2 for the triple-binary case, and Table 3 for the binary-binary case.

Because there are a large number of possible outcomes in binary-binary, triple-single, and triple-binary scattering (22, 22, and 161, respectively), many of which are qualitatively similar, we group these outcomes into broad classes. In the case of triple-single scattering we define six classes: (1) flybys, in which the hierarchical structure of the system remains the same, although the orbital parameters may have changed; (2) exchanges, in which the interloping star replaces one of the stars in the triple; (3) double binary formation, in which one star of the triple is ionized and binds to the interloping star; (4) single ionization, in which one star from the triple is ionized, leaving a binary and two unbound stars; (5) full ionization, in which all stars become unbound

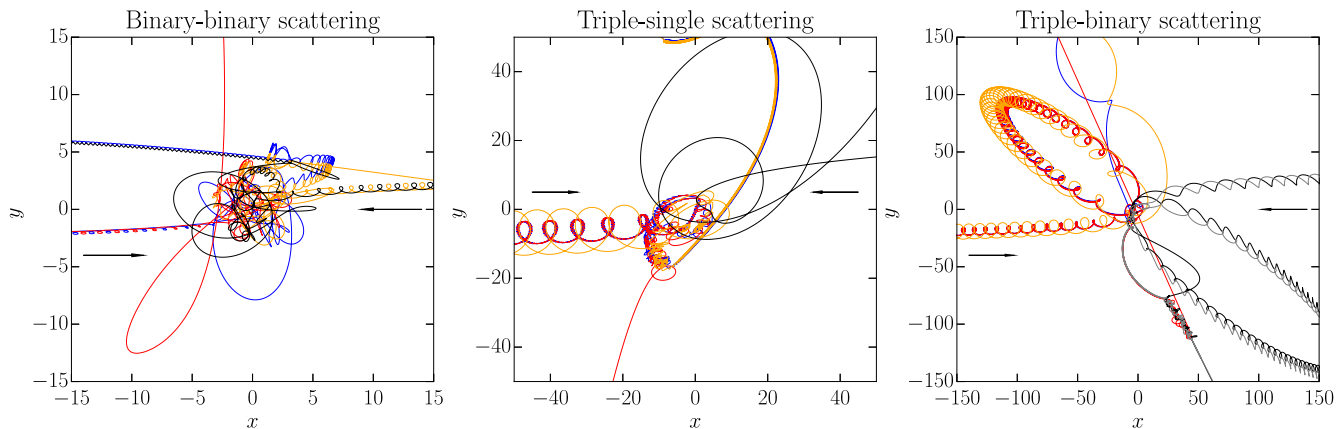


Figure 2. A sample binary-binary, triple-single, and triple-binary scattering experiment projected onto the xy -plane. The incoming velocity is $0.1v_{\text{crit}}$ in the case of triple scattering and $0.2v_{\text{crit}}$ in the case of binary-binary scattering. The semi-major axis ratio of the triple in the case of triple scattering is 10 and the semi-major axis of the incoming binary is equal to the semi-major axis of the outer binary in the case of triple-binary scattering. In the case of binary-binary scattering the triple approaches from the left and the interloping systems approaches from the right. *Left panel:* In this binary-binary scattering event one star from each binary combine to form a new binary, and the two remaining stars are ejected. *Middle panel:* In this triple-single scattering event one star from the inner binary of the triple is ejected and the interloping star is captured as a tertiary. *Right panel:* In this triple-binary scattering event one star from the inner binary is ejected, leaving two binaries and a single star.

Table 1. Normalized cross sections for the outcomes of triple-single scattering (see equation 2 for the normalization). The initial conditions are described in Section 3 and the initial hierarchy is $[[0\ 1]\ 2]\ 3$. We present both the statistical uncertainty and the systematic uncertainty. Note that the systematic uncertainty only represents an uncertainty toward larger cross sections. That is, the cross sections presented are lower limits and may be larger by the systematic uncertainty—see Section 2.2. We only present cross sections for which the statistical uncertainty is less than 50 per cent. The cross section for the outcome equal to the initial hierarchy (i.e., a flyby) is not well defined and so is not included. Such interactions can change the orbital parameters of the triple system, however, and are discussed in Section 5.1. The outcome classes are defined in Section 3.2. We also note if the scattering event produces a new triple with a hierarchy distinct from the original hierarchy.

TRIPLE-SINGLE			
Outcome	$\hat{\sigma}$	$\Delta_{\text{stat}}\hat{\sigma}$	Outcome class
$[0\ 1]\ 3\ 2$	1.309	0.013	Single ionization
$[0\ 2]\ 1\ 3$	0.092	0.003	Single ionization
$0\ [1\ 2]\ 3$	0.080	0.003	Single ionization
$0\ [1\ 3]\ 2$	0.076	0.003	Exchange ionization
$[0\ 3]\ 1\ 2$	0.074	0.003	Exchange ionization
$[[0\ 1]\ 3]\ 2$	0.033	0.002	Exchange, new triple
$[[0\ 3]\ 2]\ 1$	0.027	0.002	Exchange, new triple
$0\ [[1\ 3]\ 2]$	0.021	0.002	Exchange, new triple
$[0\ 1]\ [2\ 3]$	0.017	0.001	Double binary
$[0\ 2]\ [1\ 3]$	0.011	0.001	Double binary
$3\ [[1\ 2]\ 0]$	0.010	0.001	Scramble, new triple
$[0\ 3]\ [1\ 2]$	0.010	0.001	Double binary
$[[0\ 2]\ 1]\ 3$	0.008	1e-03	Scramble, new triple
$0\ 1\ [2\ 3]$	0.005	8e-04	Exchange ionization
$\Delta_{\text{sys}}\hat{\sigma}$	0.032	0.002	

from each other; and (6) a scramble, in which the tertiary exchanges with one of the stars of the inner binary.

In the case of binary-binary scattering we define six classes: (1) flybys, defined as in the triple-single case; (2) exchanges, in which one star from each binary exchanges places with the other; (3) triple formation, in which a stable triple is formed, leaving a single unbound star; (4) single ionization, in which one star is ionized, leaving a binary and two unbound stars; (5) full ionization, defined as in the triple-single case; and (6) exchange + ionization, in which one star from each binary binds to form a new binary, and the two other stars remain unbound.

In the case of triple-binary scattering we define seven classes: (1) flybys, defined as in the triple-single case; (2) exchanges, in which one star from the interloping binary exchanges with one star from the interloping binary; (3) double binary formation, in which one star from the triple is ionized, resulting in two binaries and an unbound star; (4) binary disruption, in which the two stars of the interloping binary become unbound; (5) triple disruption, in which the three stars of the triple become unbound from each other; (6) quadruple formation, in which one star from the interloping binary becomes bound to the triple, forming a quadruple; (7) and a scramble, defined as in the triple-single case.

Note that in triple-single and triple-binary scattering several of these outcome classes produce a ‘new’ triple (i.e., the final hierarchy differs from the original hierarchy). (In binary-binary scattering triple formation is its own class and is mutually exclusive with the other classes.) The cross sections for these classes for triple-single, triple-binary, and binary-binary scattering are displayed in Table 4. We include there the cross section for new triple formation, though for triple-single and triple-binary scattering it is not independent of the cross sections for other outcome classes.

In the case of triple scattering the systematic uncertainty is dominated by marginally unstable triples (according to Equation 14) for which the integration time exceeded

Table 2. Normalized cross sections for the outcomes of triple-binary scattering (see equation 3 for the normalization). The initial conditions are described in Section 3 and the initial hierarchy is $[[0\ 1]\ 2]\ [3\ 4]$. We present both the statistical uncertainty and the systematic uncertainty. Note that the systematic uncertainty only represents an uncertainty toward larger cross sections. That is, the cross sections presented are lower limits and may be larger by the systematic uncertainty—see Section 2.2. We only present cross sections for which the statistical uncertainty is less than 50 per cent. Flyby outcomes are not included. Such interactions can change the orbital parameters of the triple system, however, and are discussed in Section 5.1. The outcome classes are defined in Section 3.2. We also note if the scattering event produces a new triple with a hierarchy distinct from the original hierarchy.

TRIPLE-BINARY			
Outcome	$\hat{\sigma}$	$\Delta_{\text{stat}}\hat{\sigma}$	Outcome class
[0 1] 4 2 3	1.110	0.016	Double ionization
[0 1] [3 4] 2	0.990	0.015	Double binary
[[0 1] 2] 4 3	0.911	0.015	Binary disruption
[0 1] 3 [2 4]	0.072	0.004	Double binary
[0 1] 4 [2 3]	0.070	0.004	Double binary
[0 2] 1 4 3	0.048	0.003	Double ionization
0 [1 2] [3 4]	0.048	0.003	Double binary
0 [1 2] 4 3	0.048	0.003	Double ionization
[0 2] 1 [3 4]	0.045	0.003	Double binary
[[0 1] 4] 3 2	0.025	0.002	Bin. disruption, new triple
0 [1 3] 2 4	0.025	0.002	Double ionization
[0 4] 1 2 3	0.022	0.002	Double ionization
[[0 1] 3] 4 2	0.021	0.002	Bin. disruption, new triple
[0 3] 1 2 4	0.021	0.002	Double ionization
0 [1 4] 2 3	0.018	0.002	Double ionization
[[0 1] 3] [2 4]	0.011	0.002	Exchange, new triple
[[0 1] 4] [2 3]	0.011	0.002	Exchange, new triple
[[0 2] 1] [3 4]	0.006	0.001	Scramble, new triple
[[0 3] 2] 1 4	0.005	0.001	Bin. disruption, new triple
[0 4] [1 3] 2	0.005	0.001	Double binary
[3 4] [[1 2] 0]	0.005	0.001	Exchange, new triple
0 1 [2 3] 4	0.004	1e-03	Double ionization
0 1 2 [3 4]	0.004	1e-03	Double ionization
[0 3] [1 2] 4	0.004	1e-03	Double binary
[[0 2] 1] 3 4	0.004	9e-04	Bin. disruption, new triple
[[0 4] 2] 1 3	0.004	9e-04	Bin. disruption, new triple
3 [[1 2] 0] 4	0.004	9e-04	Bin. disruption, new triple
0 [[1 3] 2] 4	0.003	9e-04	Bin. disruption, new triple
[0 2] [1 3] 4	0.003	9e-04	Double binary
[0 4] [1 2] 3	0.003	9e-04	Double binary
[0 3] [1 4] 2	0.003	9e-04	Double binary
[[0 4] 3] 1 2	0.003	8e-04	Bin. disruption, new triple
0 1 [2 4] 3	0.003	8e-04	Double ionization
0 [[1 4] 2] 3	0.003	8e-04	Bin. disruption, new triple
[0 2] [1 4] 3	0.002	7e-04	Double binary
0 [[1 4] 3] 2	0.002	7e-04	Bin. disruption, new triple
[0 3] 1 [2 4]	0.002	7e-04	Double binary
[0 2] [[1 4] 3]	0.002	7e-04	Exchange, new triple
[0 4] 1 [2 3]	0.002	7e-04	Double binary
[0 4] [[1 3] 2]	0.001	6e-04	Exchange, new triple
[[0 3] 2] [1 4]	0.001	6e-04	Exchange, new triple
0 [1 3] [2 4]	0.001	6e-04	Double binary
[[0 4] 2] [1 3]	0.001	5e-04	Exchange, new triple
[0 3] [[1 4] 2]	0.001	5e-04	Exchange, new triple
[[0 2] 3] 1 4	0.001	5e-04	Bin. disruption, new triple
0 [[1 3] 4] 2	0.001	5e-04	Bin. disruption, new triple
3 [[1 4] 0] 2	0.001	5e-04	Bin. disruption, new triple
[[0 3] 4] 1 2	0.001	5e-04	Bin. disruption, new triple
[[0 4] 1] 3 2	0.001	5e-04	Bin. disruption, new triple

Table 3. Normalized cross sections for the outcomes of binary-binary scattering. The initial conditions are described in Section 3 and the initial hierarchy is $[0\ 1]\ [2\ 3]$. The cross sections have been normalized to the sum of the areas of the two binaries. We present both the statistical uncertainty and the systematic uncertainty. Note that the systematic uncertainty only represents an uncertainty toward larger cross sections. That is, the cross sections presented are lower limits and may be larger by the systematic uncertainty—see Section 2.2. We only present cross sections for which the statistical uncertainty is less than 50%. The cross section for the outcome equal to the initial hierarchy (i.e., a flyby) is not well defined and so is not included.

BINARY-BINARY			
Outcome	$\hat{\sigma}$	$\Delta_{\text{stat}}\hat{\sigma}$	Outcome class
0 1 [2 3]	1.335	0.016	Single ionization
[0 1] 3 2	1.310	0.016	Single ionization
[0 2] 1 3	0.829	0.013	Exchange ionization
[0 3] 1 2	0.823	0.013	Exchange ionization
0 [1 3] 2	0.807	0.013	Exchange ionization
0 [1 2] 3	0.800	0.013	Exchange ionization
[0 2] [1 3]	0.152	0.005	Exchange
[0 3] [1 2]	0.150	0.005	Exchange
[[0 3] 2] 1	0.003	8e-04	Triple formation
[[0 1] 2] 3	0.002	6e-04	Triple formation
[[0 3] 1] 2	0.002	6e-04	Triple formation
0 [[1 2] 3]	0.002	6e-04	Triple formation
0 [[1 3] 2]	0.002	6e-04	Triple formation
[[2 3] 0] 1	0.002	6e-04	Triple formation
[[0 2] 1] 3	0.002	6e-04	Triple formation
2 [[1 3] 0]	0.002	6e-04	Triple formation
[[0 2] 3] 1	0.001	5e-04	Triple formation
[[0 1] 3] 2	0.001	5e-04	Triple formation
3 [[1 2] 0]	0.001	5e-04	Triple formation
0 [[2 3] 1]	0.001	5e-04	Triple formation
$\Delta_{\text{sys}}\hat{\sigma}$	0.002	0.001	

the one-hour CPU time limit; 0.0263 per cent of the triple-single scattering experiments failed to complete, and of these 81 per cent failed to complete due to the CPU time limit (the rest failed because they violated the energy conservation limit). Because the Mardling stability criterion of equation (14) is not a hard boundary (Petrovich 2015) it is possible that these triples are, in fact, stable and should be classified as flybys. If, however, they are unstable on longer timescales than our integrations permit they should be classified as single ionization events since no other outcome is possible. Thus the systematic uncertainty of triple scattering should be considered as an uncertain contribution to the cross section for single ionization. In the case of binary-binary scattering the systematic uncertainty is dominated by systems that violated the energy conservation criterion during an extremely close passage. This is a much rarer occurrence than the formation of a marginally unstable triple during a triple scattering event, so the systematic uncertainty of binary-binary scattering is much lower than that of triple scattering (0.0012 per cent of systems failed to resolve, of which all were due to violations of the energy conservation limit).

Table 4. Cross sections for outcome classes in triple-single, triple-binary, and binary-binary scattering at $\hat{v} = 1$. Cross sections for “Exchange + ionization” are not included in either “Exchange” or “Single ionization.” However, the cross sections for new triples are not independent of the other cross sections. (I.e., they are a sum of subsets from the other classes.) See Section 3.2 for definitions of the outcome classes.

TRIPLE-SINGLE		
Outcome class	$\hat{\sigma}$	$\Delta_{\text{stat}}\hat{\sigma}$
Exchange	0.082	0.003
Single ionization	1.481	0.013
Full ionization	0.000	0.000
Double binary formation	0.038	0.002
Exchange + ionization	0.155	0.004
Scramble	0.018	0.001
New triple	0.100	0.003
$\Delta_{\text{sys}}\hat{\sigma}$	0.032	0.002
TRIPLE-BINARY		
Exchange	0.036	0.003
Quadruple formation	0.000	2e-04
Scramble	0.006	0.001
Binary disruption	0.996	0.016
Double binary formation	1.250	0.017
Triple disruption	1.303	0.018
Full ionization	0.000	2e-04
New triple	0.127	0.006
$\Delta_{\text{sys}}\hat{\sigma}$	0.045	0.003
BINARY-BINARY		
Exchange	0.302	0.008
Triple formation	0.020	0.002
Single ionization	2.646	0.023
Full ionization	0.000	0.000
Exchange + ionization	3.259	0.025
$\Delta_{\text{sys}}\hat{\sigma}$	0.002	0.001

3.2 Dependence on initial parameters

We next explore the dependence of the cross sections on the initial parameters of the system. In particular we separately vary the semi-major axis ratio, the incoming velocity, the eccentricities, and the masses.

3.2.1 Semi-major axis ratio

We first vary the semi-major axis ratio from $\alpha \equiv a_2/a_1 = 10^{0.6} - 10^2$. At choices of α much below our lower limit the triples become unstable and at choices of α much larger than our upper limit the computational time becomes prohibitively long because the time step is set by the orbital period of the inner binary, but the crossing time is set by the size of the outer orbit. We hold all other parameters (e.g., eccentricities, masses) fixed to their values in the model system (Section 3.1). The normalized cross sections for binary-binary, triple-single, and triple-binary scattering are shown in Fig. 3. Single ionization is the dominant outcome of triple-

single scattering for all α . At the low- α end this is because the triples are only marginally stable so minor perturbations from the interloper tend to ionize one member of the triple. At the high- α end this is because the tertiary becomes weakly bound to the inner binary. Weak perturbations from the interloper are therefore likely to ionize the tertiary. Other classes of outcomes generally require some interaction with the stars of the inner binary. The probability of such an interaction scales with the orbital area of the inner binary, so we observe that $\hat{\sigma} \propto \alpha^{-2}$.

For the case of triple-binary scattering we fix the initial value of a_1 to be equal to a_2 as we vary the semi-major axis, α . At large α , binary disruption is the dominant outcome whereas at small α double binary formation dominates. In the low- α limit the triple comes closer to instability, so single ionization from the triple is also likely to occur in addition to the disruption of the interloping binary, leading to double binary formation. In the large α case the scattering problem approaches that of binary-binary scattering in which one binary is more massive than the other. Earlier experiments have shown (e.g., Fregeau et al. 2004) that the less massive binary is more likely to be disrupted, in accordance with our results here. In this limit we might naïvely expect no dependence on α since we fix $a_1 = a_2$. Instead we observe a dependence of $\sigma \propto \alpha^{-1}$. This is because as α increases the incoming velocity (which, in the large- α limit is comparable to the orbital velocity of the inner binary of the triple) becomes larger relative to the orbital velocities of the outer binary and interloping binary. In the limit of large incoming velocities $\hat{\sigma} \propto \hat{v}^{-2}$ (Hut & Bahcall 1983), and since $\hat{v} \propto a^{-1/2}$, we have that $\hat{\sigma} \propto a_{11} \propto \alpha^{-1}$. For the same reason the scaling of the single ionization cross section in triple-single scattering exhibits the same dependence.

3.2.2 Eccentricity

We next vary the eccentricity of binaries in the systems, both individually and together while holding constant all other parameters (e.g., semi-major axis ratio and masses). To increase the range over which we can vary the outer eccentricity in triple scattering we set the outer semi-major axes to 20 AU (i.e., we use α of 20 instead of 10 as before). We vary the outer eccentricity of the triples (e_1) from 0 to 0.7 and the eccentricity of the inner binary (e_{11}) from 0 to 0.98. Even with the larger value of α at outer eccentricities larger than ~ 0.7 the triple violates the Mardling stability criterion (equation 14). In the case of triple-binary scattering we fix $e_1 = e_2$. In the case of binary-binary scattering we vary the eccentricities of either one binary or both binaries from 0 to 0.98. The cross sections for triple-single, triple-binary, and binary-binary scattering are shown in Fig. 4. In the case of binary-binary scattering the cross sections are completely independent of the eccentricity. In the case of triple scattering the cross sections are independent of the inner eccentricity and are generally independent of the outer eccentricity, although there is a modest increase in the cross section for single ionization in the case of triple-scattering and in the cross section for double binary formation in the case of triple-binary scattering.

The physical mechanism behind these dependences is twofold. First, there is some baseline cross section for the outcome which is independent of any eccentricity.

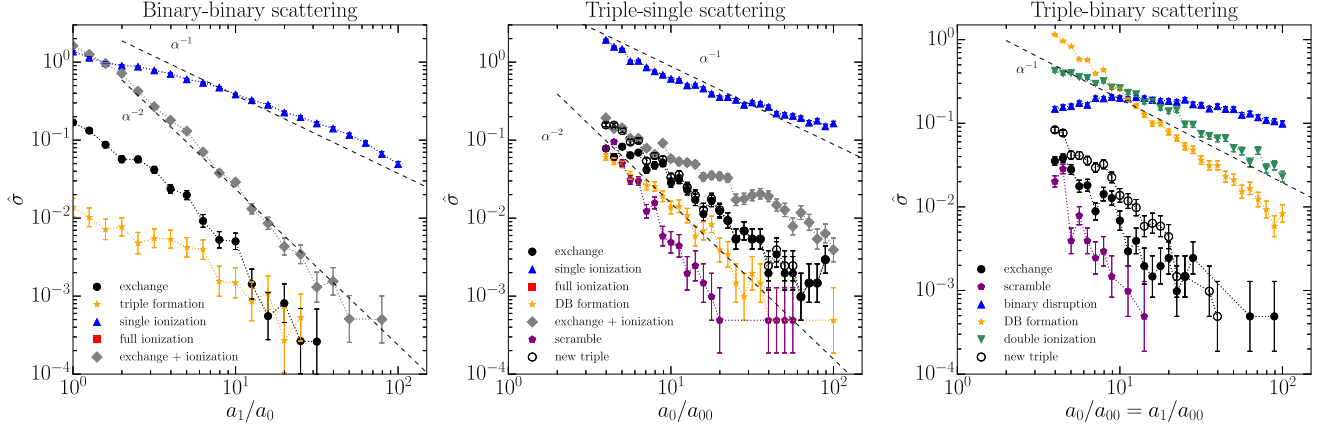


Figure 3. Cross sections of various classes of outcomes as a function of semi-major axis ratio, α , for binary-binary (left panel), triple-single, (middle panel), and triple-binary (right panel) scattering. In the limit of large semi-major axis ratios for triple-single scattering, interactions involving the inner binary should scale like the area of the inner orbit (i.e., an inverse square dependence on the semi-major axis). Indeed, the cross sections for scrambles and exchange + ionization (both of which require the interloper interact with the inner binary) are consistent with the inverse square dependence shown (black dashed line). Single ionization is the dominant outcome of triple-single scattering at all semi-major axes. At small α the triple becomes unstable to ionization from weak perturbations due to the interloper and at large α the tertiary is weakly bound relative to the inner binary so weak perturbations from the interloper lead to ionization. See Section 3.2.1 for a discussion of the origin of the α dependence of different cross sections.

Hut & Bahcall (1983) argue that this is because the cross sections for a particular orbit are only dependent on the average velocity of the orbit, which is independent of the eccentricity as a result of the virial theorem. This baseline cross section applies to all outcomes. Second, in the case of triple scattering there is an additional contribution to the cross section of ionization-like outcomes (i.e., single ionization in the case of triple-single scattering and double binary formation in the case of triple-binary scattering) due to perturbations to the eccentricity of the outer orbit of the triple, e_1 . If e_1 exceeds some critical eccentricity, e_{crit} , the triple will violate the Mardling stability criterion and will become unstable. As we show in Section 5.1, and in particular in panels b) of Fig. 10, the logarithm of the cross section for cumulative changes in the eccentricity follows the inverse of the Gompertz function:

$$\Delta e_1 = \exp(-c_1 \exp(c_2 \ln \hat{\sigma})) = \exp(-c_1 \hat{\sigma}^{c_2}), \quad (15)$$

where c_1 and c_2 are positive constants. This implies that the cross section to undergo an ionization-like reaction takes the form

$$\hat{\sigma} = \hat{\sigma}_0 + (-c_1^{-1} \ln(e_{\text{crit}} - e_1))^{1/c_2}, \quad (16)$$

where $\hat{\sigma}_0$ is the baseline cross section described above. Taking e_{crit} from the Mardling stability criterion ($e_{\text{crit}} \approx 0.733$), we find an excellent match between this functional form and the cross sections for ionization-like outcomes in Fig. 4. Best-fitting parameters are shown in Table 5.

Because e_{in} does not influence the stability of the triple, we do not see a similar effect when e_{in} is varied. This result that the cross sections are independent of the eccentricities, except when related to the stability of the triple, is consistent with the results of binary-single scattering experiments, which have also found that cross sections are independent of eccentricity (e.g., Hut & Bahcall 1983). We note, however, that is only the cross sections of strong interactions

Table 5. Best-fitting parameters of the eccentricity cross sections in Fig. 4 to the inverse Gompertz function. See equation (16) for the definition of the parameters.

Scattering type	panel	$\hat{\sigma}_0$	c_1	c_2
Triple-single	b	0.35	6.21	0.57
Triple-single	c	0.34	6.05	0.60
Triple-binary	b	0.23	3.45	0.35
Triple-binary	c	0.14	4.88	0.39

that are independent of eccentricity. Heggie & Rasio (1996) found that the magnitude of small secular perturbations to the eccentricity of a binary from a distant flyby is proportional to $e\sqrt{1-e^2}$.

3.2.3 Mass ratio

We show in Fig. 5 the effect of changing the mass of one component of the system in binary-binary, triple-single, and triple-binary scattering. In the case of triple scattering the mass of one component of the inner binary of the triple is varied. All other parameters (e.g., α , eccentricities, and $\hat{\nu}$) are held fixed. The mass of the one star is varied from $0.03 M_{\odot}$ to $40 M_{\odot}$. For small mass ratios (i.e., as the test particle limit is approached) the cross section for all outcomes in triple scattering increases by roughly an order of magnitude. In the high mass limit single ionization becomes the dominant outcome of binary-binary scattering, rising roughly with the square root of mass, and binary disruption becomes the dominant outcome of triple-binary scattering with roughly the same mass dependence. Conversely, although single ionization is the dominant outcome at high mass for triple-single scattering, the cross section decreases, nearly with the square of the mass.

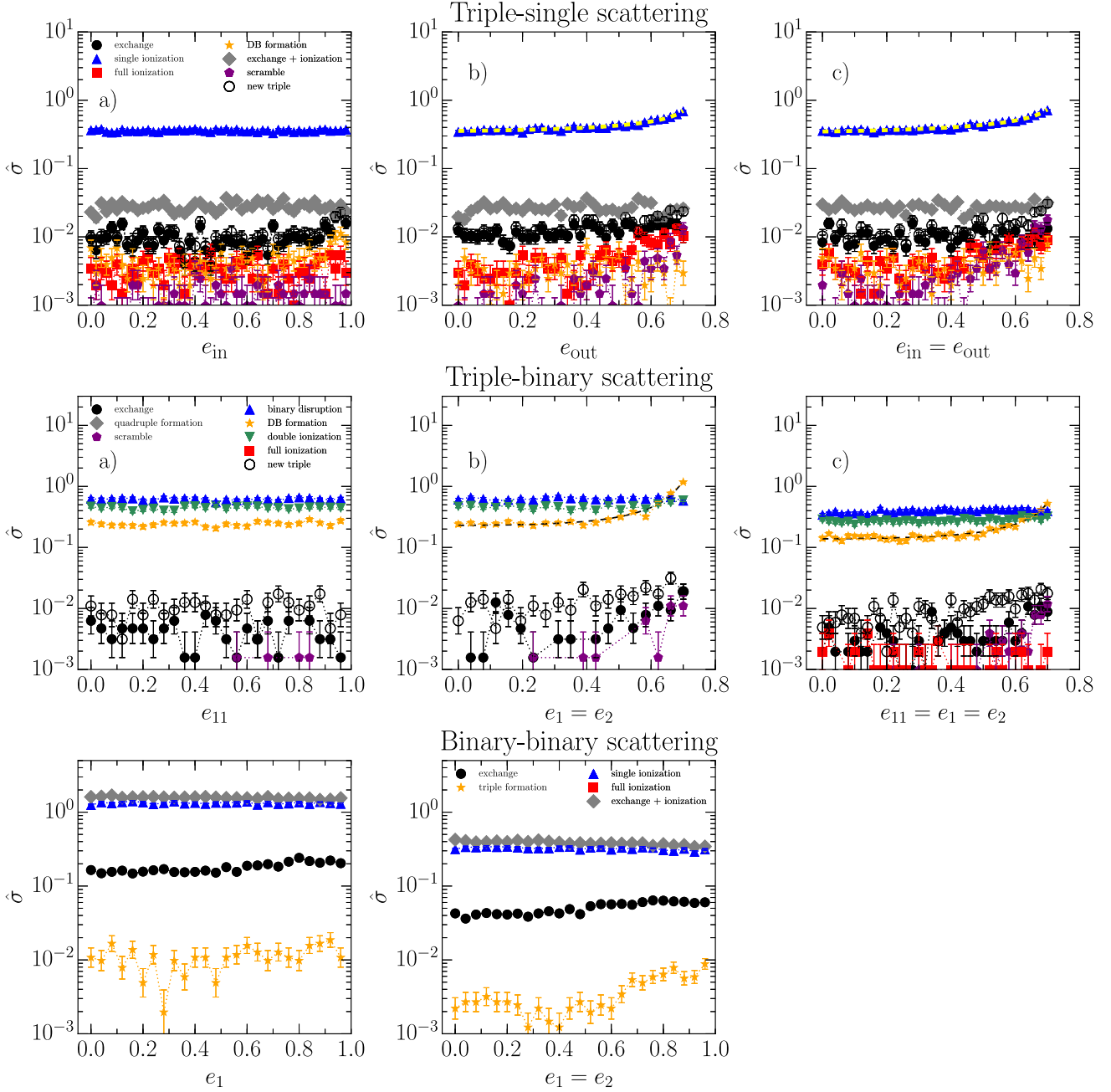


Figure 4. Cross sections of outcome classes for triple-single (top row), triple-binary (middle row), and binary-binary (bottom row) scattering as a function of eccentricity. For triple scattering we vary the inner eccentricity alone (panels a), the outer eccentricity alone (panels b), and the inner and outer eccentricities simultaneously (panels c). In the case of triple-binary scattering we set the eccentricity of the incoming binary to be equal to that of the tertiary. In the case of binary-binary scattering we vary the eccentricity of one binary only (left panel) and both binaries simultaneously (right panel). In binary-binary scattering the cross sections are independent of the eccentricities. In triple scattering the cross sections are independent of the inner eccentricity and are independent of the outer eccentricity for small outer eccentricities. At large outer eccentricities there is a small increase in the cross section for single ionization in triple-single scattering and double ionization in triple-binary scattering. This is because these triples start closer to the Mardling instability boundary, so small perturbations to the outer eccentricity can destabilize them. We fit these cross sections with the functional form of equation (16) (dashed lines) and find excellent agreement. The best-fitting parameters are shown in Table 5.

Hut (1983) derived the mass dependence of the ionization cross section for binary-single scattering in the large \hat{v} limit and found it to be proportional to m^{-2} when the most massive body resides in the binary and proportional to m^2 when the most massive body is the interloping star (see equation 17). In the large mass limit of binary-binary and triple-binary scattering, the mass dependence should be similar to the case of binary-single scattering with a massive interloping star. Likewise, the case of triple-single scattering should exhibit a similar mass dependence to binary-single scattering with a massive binary. However, we are not in the high velocity limit ($\hat{v} = 1$) so we expect the mass dependencies to soften, which is what we observe. Nevertheless, the trend of increased ionization cross sections for low-mass interloping binaries and decreased ionization cross sections for low-mass interloping single stars holds even in the moderate velocity regime.

3.2.4 Incoming velocity

We finally examine the effect of the velocity at infinity of the interloping system. We measure these velocities relative to the critical velocity of the system (see equations 11 and 12) and explore a range of two dex centered around v_{crit} . It is difficult to explore a much larger range because velocities much larger than $10v_{\text{crit}}$ yield very small cross sections and therefore have large statistical uncertainties. Velocities much smaller than $0.1v_{\text{crit}}$ require an excessive amount of computing time because the low total energy of the system means that it takes a long time for the system to random walk to a region of phase space where one object has a sufficient amount of energy to escape and leave behind a stable system.

The cross sections are presented in Fig. 6. Hut (1983) found two high-velocity limits in binary-single scattering: the cross section for ionization, which has a dependence of $\hat{\sigma} \propto \hat{v}^{-2}$ and the cross section for exchange, which has a dependence of $\hat{\sigma} \propto \hat{v}^{-6}$. Although there are many more possible outcomes in binary-binary, triple-single, and triple-binary scattering, the behavior of the cross sections is qualitatively similar to binary-single scattering, in that at high velocity the outcomes may be grouped into those with a \hat{v}^{-2} dependence (“ionization-like” outcomes), and those with a steeper dependence (“exchange-like” outcomes). In some cases exchange-like outcomes follow the same \hat{v}^{-6} dependence as in binary-single scattering (e.g., triple formation in binary-binary scattering and quadruple formation in triple-binary scattering), but in others the velocity dependence is shallower (e.g., exchanges in binary-binary scattering, which display a \hat{v}^{-4} dependence). We discuss these results in more detail in Section 4.2.

4 ANALYTIC APPROXIMATIONS

We here develop analytic approximations to the cross sections computed in Section 3. We first review binary-single scattering, and then generalize the theory of binary-single scattering to four-body scattering.

4.1 Three-body scattering

The analytic theory of binary-single scattering of point masses was developed by Heggie (1975) and Hut (1983) and has been found to agree with numerical scattering experiments quite well (Hut & Bahcall 1983). Although the derivation is complicated, the results are straightforward to summarize. In binary-single scattering of point masses only three classes of outcomes are possible: (1) a flyby, (2) an exchange, or (3) an ionization. It is not possible to form a stable triple from binary-single scattering (Chazy 1929; Littlewood 1952; Heggie 1975; Heggie & Hut 2003). The cross section of a flyby is not well defined, but Hut (1983) explicitly calculated the cross section for the other two classes in the high velocity limit ($\hat{v} \gg 1$) and found them to be

$$\hat{\sigma}_{\text{ion}} = \frac{40}{3} \frac{m_3^2}{m_{11}m_{12}(m_{11} + m_{12} + m_2)} \frac{1}{\hat{v}^2}, \quad \hat{v} \gg 1 \quad (17)$$

and

$$\hat{\sigma}_{\text{ex}} = \frac{20}{3} \frac{m^2(m + m_2)^4}{m_3^2(2m + m_2)^3} \frac{1}{\hat{v}^6}, \quad \hat{v} \gg 1 \quad (18)$$

where the latter is only valid for equal mass binaries, $m \equiv m_{11} = m_{12}$. Hut (1983) found that both cross sections are independent of eccentricity.

In the low velocity limit ($\hat{v} \ll 1$) the cross sections cannot be computed with precise numerical coefficients. Nevertheless, the velocity scaling in the low velocity case is simple because ionization is not possible and the only mechanism to change the cross section is gravitational focusing. This is because at low velocities the speed of the interloping star when it is close enough to interact strongly with the binary will be very close to the escape speed. Thus for any low velocity system, the incoming velocities when the system begins strong interactions will be nearly the same, and the cross section will scale as

$$\hat{\sigma} \propto \frac{1}{\hat{v}^2}, \quad \hat{v} \ll 1. \quad (19)$$

The cross sections may be combined by taking the reciprocal of the sum of the reciprocals of the cross sections in the two extreme limits. This is because different physical effects limit the rate of production of particular outcomes and the combined effect of rate limiting processes is generally the reciprocal of the sum of the reciprocals. Because the mass terms are in general not known, we introduce normalization factors ($\hat{\sigma}_a$, $\hat{\sigma}_b$, etc.), which can be determined empirically. The cross section for exchange is then

$$\frac{1}{\hat{\sigma}_{\text{ex}}} = \frac{\hat{v}^2}{\hat{\sigma}_a} + \frac{\hat{v}^6}{\hat{\sigma}_b}. \quad (20)$$

The validity of this functional form is demonstrated in Fig. 7 where we fit equation (20) to numerical exchange cross sections (blue dashed line) for binary-single scattering of equal mass stars.

The cross section for full ionization is necessarily zero for $\hat{v} < v_{\text{crit}}$. For velocities slightly in excess of v_{crit} ($v = v_{\text{crit}} + \sqrt{2}\varepsilon$, where $\varepsilon \ll 1$), the cross section for full ionization in equal mass systems scales as (Heggie & Sweatman 1991)

$$\hat{\sigma}_{\varepsilon \ll 1} \propto \varepsilon^{\sqrt{13}-1} \propto (\hat{v} - 1)^{(\sqrt{13}-1)/2}. \quad (21)$$

Therefore the general cross section for ionization is

$$\frac{1}{\hat{\sigma}_{\text{ion}}} = \frac{(\hat{v} - 1)^{(1-\sqrt{13})/2}}{\hat{\sigma}_c} + \frac{\hat{v}^2}{\hat{\sigma}_d}. \quad (22)$$

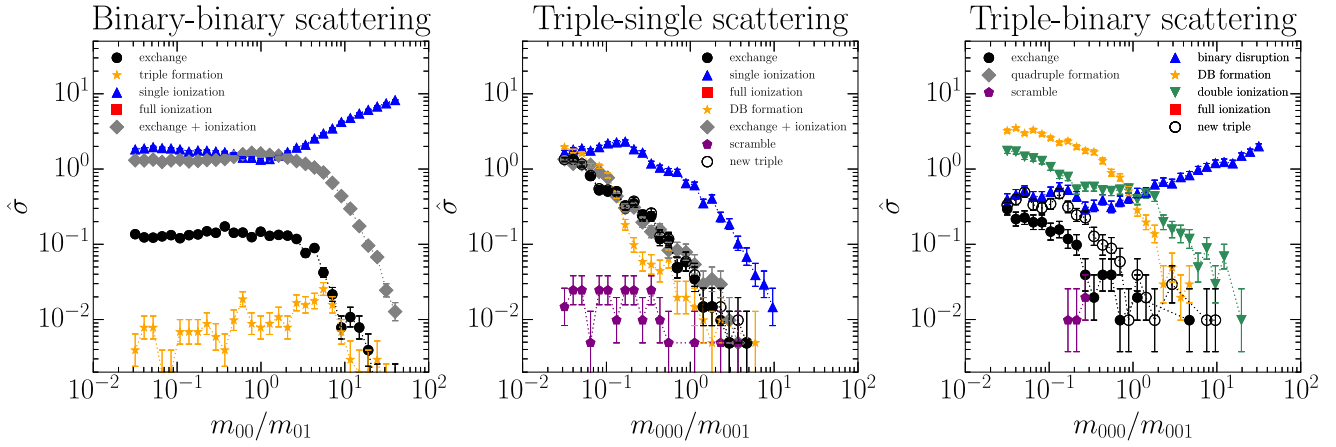


Figure 5. Cross sections of outcome classes for binary-binary (left panel), triple-single (middle panel) and triple-binary (right panel) scattering as a function of the mass ratio of one component of the binary (in the case of binary-binary scattering) or of one component of the inner binary (in the case of triple scattering) to all other components of the system. The masses of all other components of the system remain fixed and equal to each other. In the high mass limit the more massive system tends to disrupt the incoming system. This leads to an increase in the cross section for single ionization in binary-binary and triple-binary scattering. In the case of triple-single scattering all cross sections decrease because the incoming system cannot disrupt.

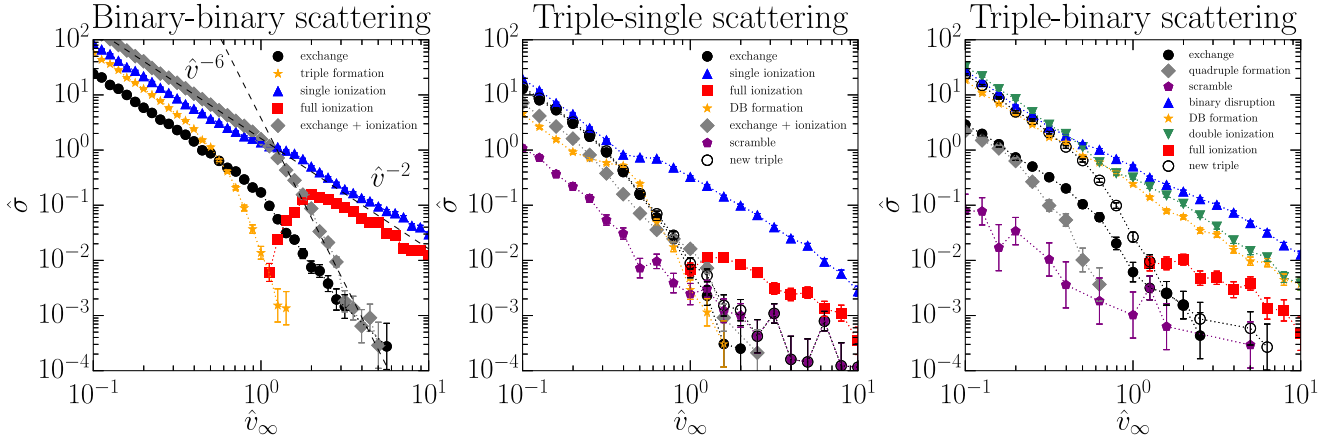


Figure 6. Cross sections of outcome classes for binary-binary (left panel), triple-single (middle panel) and triple-binary (right panel) scattering as a function of the incoming velocity. The velocities are written relative to the critical velocity of the system (see equations 11 and 12). Outcomes which require an ionization from one system follow a v^{-2} dependence at high velocities, whereas those requiring an exchange follow a steeper dependence. The kink in the cross section for single ionization is explained in Section 4.2.

Note, however, that the exponent on the $\hat{\sigma}_c$ term is only valid in the case of approximately equal masses. If one object contains more than $\sim 1/2$ of the mass, the dominant orbital configuration leading to full ionization will change, leading to a different exponent (Sweatman 2007). Sweatman (2007) lists exponents for other configurations, but this exponent could also be determined empirically. The validity of the combined cross section for ionization is also illustrated in Fig. 7 (red dashed line).

4.2 Four-body scattering

Four-body scattering can occur through binary-binary or triple-single scattering.³ Because the number of objects in-

³ In principle a simultaneous interaction between a binary and two independent single stars or a simultaneous interaction be-

interacting is the same in both cases, they generally may be studied in the same framework. Although there are 22 distinct possible outcomes of four-body scattering, we here examine the velocity dependences of three broad classes of outcomes: (1) ionization, including single and full ionization; (2) exchange; and (3) triple formation.

It is instructive to study the velocity dependence of ionization in the extreme semi-major axis ratio limit. If the semi-major axes between the two binaries are very different or the semi-major axis ratio of the triple is very large, then the problem can be considered to be a three-body scattering problem in two limits: (1) at low velocities the smaller binary can be considered a point mass and (2) at high velocities one component of the larger binary can be ignored. There are

tween four single stars are also possible, but such events are rare and so we do not study them here.

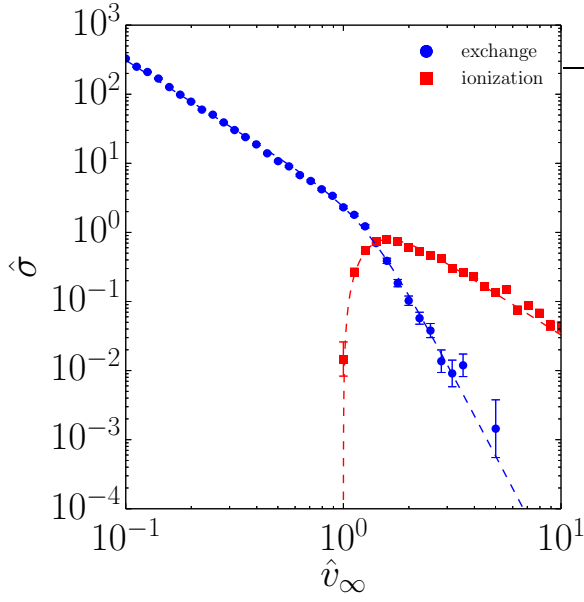


Figure 7. Normalized cross sections for exchange (blue circles) and ionization (red squares) in equal-mass binary-single scattering as a function of incoming velocity (cf. Fig. 5 of Hut & Bahcall 1983). The dashed lines are an empirical fit to equations (20) and (22). The analytic approximation is based on a combination of the low velocity limits ($\hat{v} \ll 1$ for exchange and $\hat{v} - 1 \ll 1$ for ionization) and the high velocity limits ($\hat{v} \gg 1$). Values for the normalization parameters $\hat{\sigma}_a$, $\hat{\sigma}_b$, etc. are estimated from the numerical data with best-fitting values of $\sigma_a \approx 9.76$, $\sigma_b \approx 28.9$, $\sigma_c \approx 12.8$, and $\sigma_d \approx 10.3$. The good agreement between the data and the approximation for all \hat{v} implies that the two limits capture all the relevant physics of binary-single scattering.

therefore two critical velocities in the four-body scattering problem: the critical velocity of the wide binary scattering off of interloping system, $\hat{v}_{\text{crit},1}$, and the critical velocity of the interloping system scattering off of one component of the wide binary, $\hat{v}_{\text{crit},2}$.

In the limit that the semi-major axis of the smaller binary approaches zero, the cross section for single ionization will appear like the cross section for ionization in three-body scattering given by equation (22) with the only difference being that one object in the three-body scattering event has a mass twice as great as the others because it is a binary. The effect of this is to change the exponent on the $(\hat{v} - 1)$ term from $\sqrt{13} - 1$ to $(2 + \sqrt{10})/8$ (section 4.3 of Heggie & Sweatman 1991), and to change the base from $(\hat{v} - 1)$ to $(\hat{v} - \hat{v}_{\text{crit},1})$. In the limit that the semi-major axis of one binary approaches zero the cross section for single ionization approaches zero for $\hat{v} < \hat{v}_{\text{crit},1}$. But the cross section will always be non-zero because it is possible for single ionization to occur by hardening the smaller binary. The cross section for a wide encounter with a hard binary to harden the binary enough to ionize the interloping object takes the form (Heggie 1975, equation 5.44)

$$\hat{\sigma}_{\hat{v} < \hat{v}_{\text{crit},1}} = \frac{\hat{\sigma}_a}{\hat{v}^2}, \quad (23)$$

where $\hat{\sigma}_a$ is a normalization factor and sub-linear terms (i.e., terms with only a logarithmic dependence on the velocity) have been neglected. The total cross section for single ion-

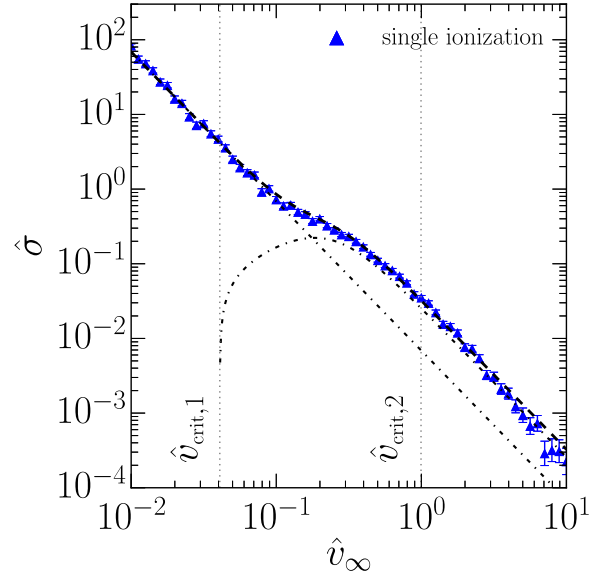


Figure 8. Cross sections for outcomes of equal mass binary-binary scattering with a semi-major axis ratio of 100 and circular orbits as a function of incoming velocity. We fit the cross sections for single ionization to equation (24) (dashed line). The best-fitting parameters are $\hat{\sigma}_a \approx 2.16 \times 10^{-2}$, $\hat{\sigma}_b \approx 3.47$, and $\hat{\sigma}_c \approx 8.08 \times 10^{-2}$. The ionization cross section consists of two components: a component similar to the full ionization cross section in binary-single scattering (curved dot-dashed line), and a component due to hardening of the inner binary (straight dot-dashed line). When summed, these two components produce a kink at velocities intermediate between $\hat{v}_{\text{crit},1}$ and $\hat{v}_{\text{crit},2}$ (dotted lines).

ization in either triple-single or binary-binary scattering is then given by

$$\hat{\sigma}_{\text{ion}} = \frac{\hat{\sigma}_a}{\hat{v}^2} + \left(\frac{(\hat{v} - \hat{v}_{\text{crit},1})^{(2+\sqrt{10})/8}}{\hat{\sigma}_b} + \frac{\hat{v}^2}{\hat{\sigma}_c} \right)^{-1}. \quad (24)$$

In Fig. 8 we present the cross section for single ionization for binary-binary scattering with a semi-major axis ratio of 100, equal masses, and circular orbits. We fit the numerical data to the functional form of equation (24) and find an excellent match. (See the caption of Fig. 8 for the best-fitting parameters.)

To study exchange and triple formation we return to more moderate semi-major axis ratios: unity for binary-binary scattering, and 10 for triple-single scattering. As discussed in Section 4.1, Hut (1983) derived the high-velocity exchange cross section to be proportional to \hat{v}^{-6} for binary-single scattering. We find from our numerical experiments in Section 3.2.4 that the high-velocity exchange cross section for exchange is shallower, being instead proportional to \hat{v}^{-4} for binary-binary and triple-single scattering (Fig. 6, black points).

In binary-binary scattering new triple formation occurs via an exchange. We find empirically that the velocity dependence for the new triple cross section is proportional to \hat{v}^{-6} in the high velocity limit for binary-binary scattering (blue points, Fig. 9). In triple-single scattering, exchanges are the dominant channel for new triple formation at low

velocities and velocities slightly larger than the critical velocity. In the high velocity limit the cross section for new triple formation via exchange is likewise proportional to \hat{v}^{-6} for triple-single scattering.

In the case of triple-single scattering new triple formation may also occur via a scramble. In the high velocity limit the cross section for scrambles is proportional to \hat{v}^{-2} (red points, Fig. 9). This is because a scramble is, in a sense, an incomplete ionization. The interloping star imparts enough energy to one star of the inner binary such that its semi-major axis becomes much larger than that of the tertiary of the original system, but not enough energy to ionize it. At low velocities a scramble is a rare outcome, but due to the shallower velocity dependence, at sufficiently high velocities it becomes the dominant mechanism by which to form new triples in triple-single scattering.

We may combine these velocity dependences to obtain the general velocity dependence of the cross section for triple formation. For binary-binary scattering, the cross section has an identical form to the exchange cross section in binary-single scattering, except that the break occurs near $\hat{v}_{\text{crit},1}$ rather than $\hat{v} = 1$ (this is reflected in the smaller best-fitting value for $\hat{\sigma}_b$):

$$\frac{1}{\hat{\sigma}_{\text{new trip.}}} = \frac{\hat{v}^2}{\hat{\sigma}_a} + \frac{\hat{v}^6}{\hat{\sigma}_b}. \quad (25)$$

For triple-single scattering the cross section is similar, except that an additional high velocity \hat{v}^{-2} term must be added to account for scrambles:

$$\hat{\sigma}_{\text{new trip.}} = \frac{\hat{\sigma}_a}{\hat{v}^2} + \left(\frac{\hat{v}^2}{\hat{\sigma}_b} + \frac{\hat{v}^6}{\hat{\sigma}_c} \right)^{-1} \quad (26)$$

We present a fit of the new triple cross section to equations (25) and (26) in Figure 9. The match between equation (25) and the binary-binary scattering cross sections is excellent. The match between equation (26) and the triple-single scattering cross sections is good, but we note that at high velocities the scramble cross section appears to be better fit with a $\hat{v}^{-3/2}$ dependence. We present this alternative velocity dependence in Figure 9 in gray. At present we do not have an analytic understanding of this shallower slope.

While the normalization parameters $\hat{\sigma}_a$, $\hat{\sigma}_b$, etc., should be determined by fitting equations (24), (25), and (26), for systems not too dissimilar from those presented in Figures 8 and 9 the ratios between the normalization parameters should be approximately constant. The overall scale can then be estimated from the dependences of the cross sections in Figures 3–5. For systems far from the systems presented in Figures 8 and 9, the normalization parameter may be quite different from these estimates because they may depend on each other in a nonlinear way.

5 ORBITAL PARAMETER DISTRIBUTIONS AFTER SCATTERING

Scattering events can affect the orbital parameter distribution of triples in two ways: by perturbing the orbital elements of an existing triple in a flyby, and by creating a new triple system. We are particularly interested in determining the distribution of orbital parameters that govern the strength and timescale of KL oscillations, namely $\cos i$, α ,

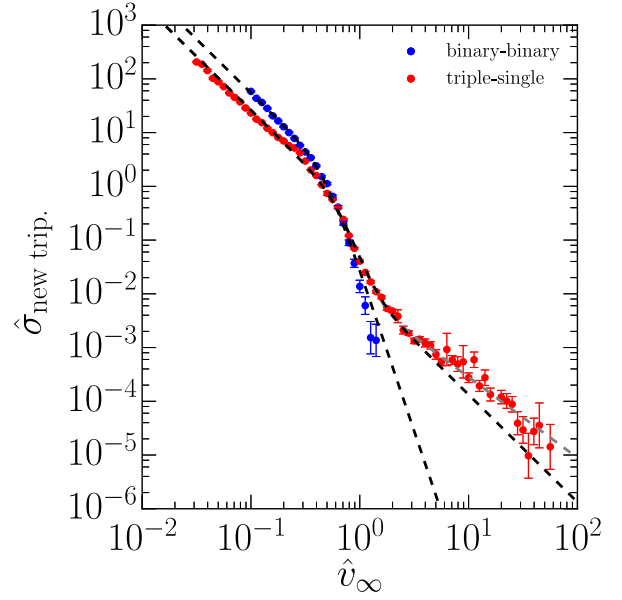


Figure 9. The velocity dependence of the cross section for new triple formation for binary-binary and triple-single scattering of our model system (see Section 3.1). We fit the velocity dependence to equations (25) and (26) (black dashed lines). At high velocities the triple formation cross section from binary-binary scattering is proportional to \hat{v}^{-6} . At velocities slightly above the critical velocity, the new triple formation cross section from triple-single scattering carries the same \hat{v}^{-6} dependence, but at higher velocities, new triple formation is dominated by scrambles, which are ionization-like and would therefore carry a \hat{v}^{-2} dependence. We note, however, that the triple-single data are better fit by a $\hat{v}^{-3/2}$ dependence (gray dashed line). For binary-binary scattering our best fitting parameters are $\hat{\sigma}_a \approx 0.567$ and $\hat{\sigma}_b \approx 0.0279$. For triple-single scattering our best fitting parameters assuming a \hat{v}^{-2} dependence for scrambles is $\hat{\sigma}_a \approx 0.247$, $\hat{\sigma}_b \approx 0.0402$, and $\hat{\sigma}_c \approx 0.0133$. Assuming a $\hat{v}^{-3/2}$ dependence for scrambles the best fitting parameters are $\hat{\sigma}_a \approx 0.257$, $\hat{\sigma}_b \approx 0.044$, $\hat{\sigma}_c \approx 8.89 \times 10^{-3}$.

and e_{out} . We first examine the case of flybys in Section 5.1 and then examine newly formed triples in Section 5.2.

5.1 Changes to the orbital parameters from flybys

Cross sections for flybys are not well defined because they diverge for infinitesimally small perturbations. As such, we instead calculate the cumulative cross section, $\sigma(X > x)$, defined to be the cross section for a change in parameter X by at least x . From our experiments involving the model system (see Section 3.1) we select those which result in a flyby. We then calculate the cumulative cross section for generating changes in the orbital parameters of a given magnitude or larger. These cross sections are shown in Fig 10. The normalized cross section for inducing a change in the semi-major axis of order unity is $\hat{\sigma} \approx 0.54$, which is very close to the cross section for single ionization of 1.48. That the two cross sections should be comparable is to be expected since there is only a small difference in energy in changing α by order unity and in ionizing the object. The logarithm of the cumulative cross section for changes to e_1 is well described

by the inverse of a Gompertz function⁴ (cf. equation 15):

$$\Delta e_1 = \exp(-c_1 \exp(c_2 \ln \hat{\sigma})) = \exp(-c_1 \hat{\sigma}^{c_2}). \quad (27)$$

We present a fit to the cumulative cross sections in Fig. 10, but the difference between the two is typically smaller than the width of the lines (the best-fitting parameters are presented in the caption to Fig. 10). The cross section for large changes to the eccentricity is small ($\hat{\sigma} \ll 1$ for $1 - \Delta e_1 \ll 1$) because to remain stable such systems need to gain a large amount of energy and are therefore more likely to be ionized than remain bound. The cross section for moderate changes to the eccentricity ($\Delta e_1 \sim 0.5$) is of order unity ($\hat{\sigma} \sim 1$), similar to the case for a change in α . The cumulative cross section for changes to e_{out} drops more steeply for $\Delta e_{\text{out}} \gtrsim 0.7$. This is due to the fact that the initial triple is unstable for $e_{\text{out}} \sim 0.7$ (see equation 14). To produce $\Delta e \gtrsim 0.7$ two things are required: (1) the semi-major axis ratio must increase by enough that at the final e_{out} the triple is no longer unstable, and (2) e_{out} must change by Δe_{out} . The addition of requirement (1) induces the sharper drop in the cross section for $\Delta e_{\text{out}} \gtrsim 0.7$. To check if the form of equation (27) is independent on the assumption of equal masses we repeated the calculations used to produce panel b) of the upper row of Figure 4 and panel b) of the upper row of Figure 10 using the following sets of masses: $(m_{111}, m_{112}, m_{12}, m_2) \in \{(4, 3, 2, 1), (1, 2, 3, 4), \text{ and } (1, 10^{-6}, 1, 1)\}$. We found equation (27) to be an excellent fit in all cases. While this does not prove that equation (27) is necessarily valid for all possible mass ratios, it demonstrates that the form of equation (27) is not strongly dependent on the assumption of equal masses.

The change in the inclination is particularly interesting due to its relevance for inducing KL oscillations in a triple system. However there is a confounding effect in the cumulative cross section for this orbital parameter. Since some triples will begin at high inclinations, their inclination can change in isolation due to KL oscillations. This is a difficult effect to disentangle from changes that are solely due to scattering or perturbations from interloping stars. To estimate the magnitude of this effect, we evolve a sample of triple systems identical to those used in our model systems but without any interloping stars for the same length of time as our flyby calculations. We then calculate the cumulative distribution of the change in inclination to compare its magnitude to the distribution when an interloping star is present. Small changes in inclination can be accounted for almost entirely by KL oscillations. Because these scattering calculations complete in $\sim 10\%$ of the KL timescale, t_{KL} , KL oscillations cannot produce large changes in inclination. Thus, the cumulative cross sections for large changes in inclination are entirely due to the interloping star. In more compact systems, however, the KL timescale may be comparable to the timescale of the scattering event, in which case either scattering or KL oscillations would be able to produce large changes in inclination. The distributions of positive and negative changes in $\cos i$ are equal to within the statistical uncertainty of our results.

⁴ A Gompertz function is defined to be any function of the form

$$f(t) = ae^{-be^{-ct}},$$

where a is the asymptote and b and c are positive constants.

We additionally show the relationship between changes to the mutual inclination and changes to e_{out} in Figure 11. To demonstrate the magnitude of the effect of KL oscillations we also include the relationship between changes to the inclination and e_{out} from the isolated triples. Flyby events for which $\Delta \cos i \lesssim 10^{-2}$ do not exhibit a strong correlation between the change to the inclination and e_{out} . In these systems the dynamics of the isolated triple therefore overwhelm the contributions of the interloping star. Flyby events for which $\Delta \cos i \gtrsim 10^{-2}$ do exhibit a strong correlation between the change in the inclination and e_{out} , albeit with substantial scatter. This result is consistent with other dynamical studies (e.g., Li & Adams 2015).

5.1.1 A note on convergence

The issue of whether our calculations are converged in the maximum impact parameter, b_{max} , is subtler in flyby events than the convergence analysis presented in Section 2.3, so we revisit it here. In Section 2.3 we considered the convergence of the cross sections of outcomes from “strong” interactions (i.e., interactions for which the hierarchy changed). In flyby events, however, arbitrarily distant encounters can have arbitrarily weak dynamical effects, so our calculations can never be truly converged in b_{max} . We can, however, determine the magnitude of the change of orbital parameters down to which our calculations are converged by calculating the cumulative cross sections using a variety of b_{max} ’s. We present the results of this calculation for changes to the semi-major axis ratio, α , in Figure 12.

Our results are converged down to relative changes in α of $\sim 3 \times 10^{-3}$. The cross section for smaller changes to α diverges, however. This is due to the fact that the semi-major axes of the inner and outer orbits of an isolated triple will exhibit small variations over time. We demonstrate the scale of this variability by integrating an isolated triple in Figure 13. For the triples we are studying here the scale of this variability is $\Delta \alpha / \alpha_0 \sim 3 \times 10^{-3}$. This scale corresponds with the point at which the cross sections diverge in Figure 12. Note, however, that the scale of this variability is dependent on the on the orbital parameters of the triples being studied. In particular, as $\alpha \rightarrow \infty$, the relative size of this variability will approach zero. Calculation of the cross sections of changes to the orbital parameters from flybys of triples with very large α may therefore require a larger b_{max} than given by equation (9).

5.2 Distribution of orbital parameters in dynamically formed triples

The scattering experiments presented in Section 3 demonstrated that some fraction of binary-binary, triple-single, and triple-binary scattering events produce new triple systems. Because this fraction is relatively small, we here run three larger suites of scattering experiments to obtain better statistics on the distribution of orbital parameters of dynamically formed triples. One suite consists of binary-binary scattering experiments, another of triple-single experiments, and the last of triple-binary experiments. In the case of triple-binary scattering the interloping binary has a semi-major axis equal to the outer binary of the triple.

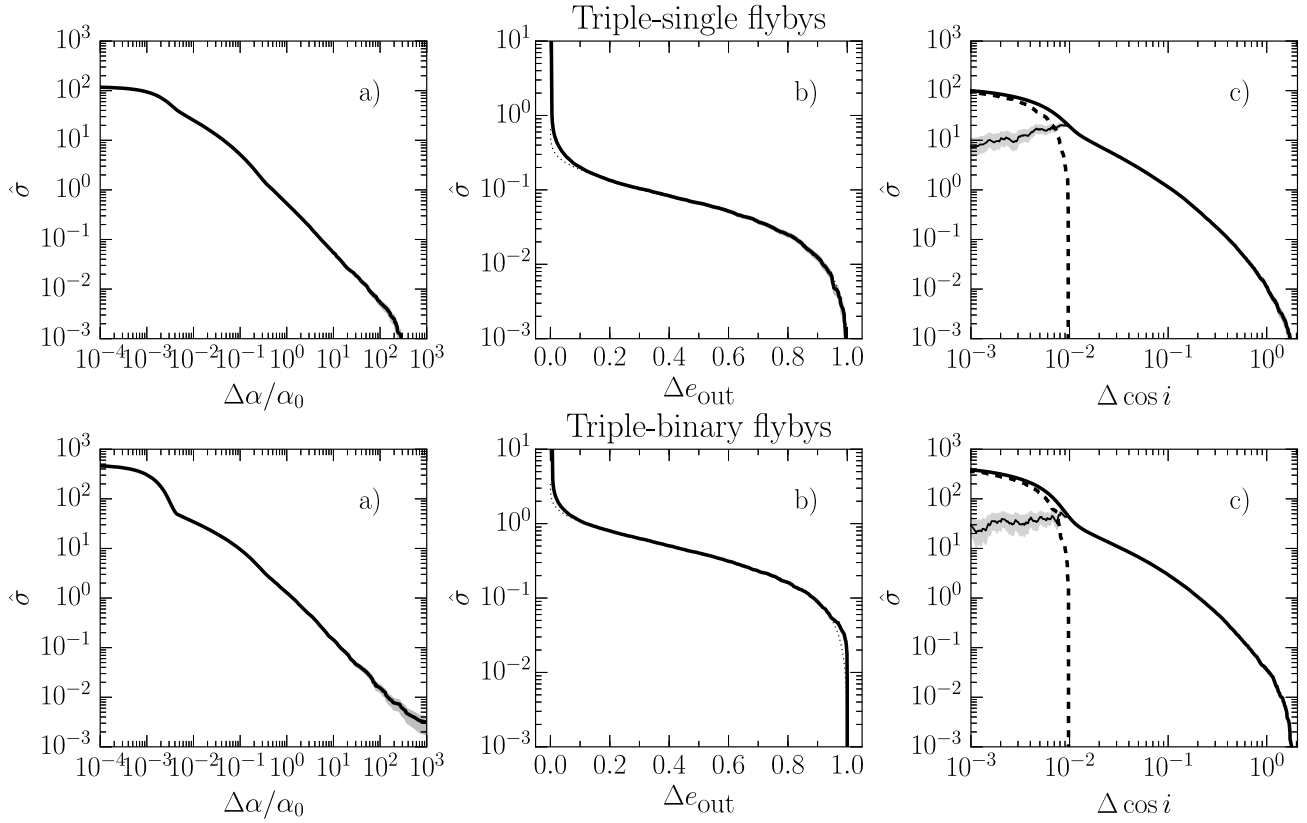


Figure 10. The cumulative cross section for changes to the orbital parameters from triple-single flybys (top row) and triple-binary flybys (bottom row) with incoming velocities of $\hat{v} = 1$. We show here changes to the semi-major axis ratio (panels a), the outer eccentricity (panels b), and the mutual inclination (panels c). The cross sections presented are the cross sections for a change in the orbital parameter of that magnitude *or greater*. The $1\text{-}\sigma$ confidence interval is shown by the gray shaded region, although typically these uncertainties are smaller than the width of the lines. We fit the Δe_1 cumulative cross sections to a Gompertz function (panels b, dotted line) and find an extremely close match. Except for very small or large Δe_1 the difference between the numerical data and the fit is smaller than the width of the line. The best-fitting parameters are $c_1 \approx 0.0626$ and $c_2 \approx 0.866$ for triple-single flybys and $c_1 \approx 0.469$ and $c_2 \approx 0.810$ for triple-binary flybys. Since isolated triples can undergo changes to their inclination due to KL oscillations (an effect which is necessarily present when we perform our scattering experiments), we compare the magnitude of this effect to the cross sections due to scattering by calculating the evolution of an identical set of triples for an identical length of time (panels c, dashed line). The difference between the scattering cross section and the cross section from the isolated triples is shown by the thin black line with $1\text{-}\sigma$ uncertainties. KL oscillations are unable to produce large changes in the inclination because the flyby timescale is much shorter than the KL timescale.

We set the semi-major axis ratio of the triples to be 10 and set $a_1 = a_2$ in the case of binary-binary scattering. We furthermore set all masses to be equal and set an incoming velocity of $v = v_{\text{crit}}$. We do not include the orbital parameters of triples resulting from flybys in these distributions as these were studied in Section 5.1. To ensure that the resulting triples are stable we run them in isolation for 100 outer orbital periods and reject those which do not maintain the same hierarchy. (E.g. we reject systems which begin in the configuration $[[0\ 1]\ 2]$ but end in the configuration $[[0\ 2]\ 1]$). This is similar to the stability test used by Mardling & Aarseth (1999).

We must be careful when calculating the inclination distribution. Because the calculations can often run for times comparable to t_{KL} , KL oscillations can bias the inclination distribution towards the Kozai angles of 39° and 141° . To correct for this we run the triples in isolation for half the length of time that the scattering event was computed; this is approximately the length of time that the triple has ex-

isted for. We then use the inclination closest to 90° in the inclination distribution because the triple spends most of its time at this inclination. (For example, an equal mass triple with an initial inclination of 85° spends over 80 per cent of its time within 10° of its initial inclination.)

The distribution of orbital parameters is shown in Fig. 14. The most important feature of these distributions is that scattering produces triples which are extremely compact, in that the ratio of the distance at periastron of the outer orbit, $r_{\text{peri, out}}$, to a_{in} is quite small, typically ~ 10 . Indeed, the vast majority of these triples are on the verge of instability.

Because these triples are so compact, they have extremely large ϵ_{oct} . This parameter is a measure of the strength of octupole-order contributions to the KL oscillations and is defined to be (Lithwick & Naoz 2011; Naoz et al. 2013)

$$\epsilon_{\text{oct}} \equiv \frac{1}{\alpha} \left(\frac{e_{\text{out}}}{1 - e_{\text{out}}^2} \right). \quad (28)$$

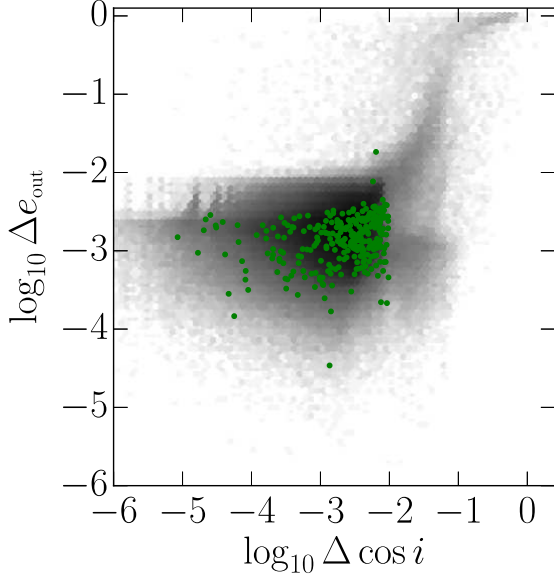


Figure 11. The relationship between changes to the mutual inclination and changes to e_{out} from flyby events. The darkness of the hexagonal bins corresponds to the number of events, binned logarithmically. To demonstrate the magnitude of KL oscillations we include this relationship for several isolated triples (green points). For events in which there is a change to $\cos i$ less than $\sim 10^{-2}$ there is not a strong correlation between $\Delta \cos i$ and e_{out} . Changes to the orbital parameters are due primarily to KL oscillations rather than the dynamical effect of the interloping star. For events in which there is a change to $\cos i$ greater than $\sim 10^{-2}$ there is a strong correlation between $\Delta \cos i$ and Δe_{out} , though with substantial scatter.

Triples with larger e_{oct} have stronger eccentric KL oscillations. In particular, Lithwick & Naoz (2011) note that for $e_{\text{oct}} > 10^{-2}$ the parameter space for orbital flips (and hence arbitrarily large eccentricities in the inner binary) widens dramatically. Our results indicate that nearly all dynamically formed triples have $e_{\text{oct}} > 10^{-2}$. We note that the particular triples formed from these experiments do not undergo typical eccentric KL oscillations because they are of equal mass, so the octupole order terms of the Hamiltonian vanish (e.g., Ford et al. 2000). Nevertheless, in extremely compact triples non-secular effects can drive the inner binary to arbitrarily large eccentricities (e.g., Antonini et al. 2014; Bode & Wegg 2014; Antognini et al. 2014). Moreover, as we show in Section 5.3, these results for the dynamical formation of triples are generic and apply to unequal mass triples.

The inclination distributions appear to be approximately uniform, but are clearly biased towards inclinations less than 90° , i.e., prograde orbits. This is curious because we began with a distribution of inclinations uniform in $\cos i$ (i.e., as many retrograde orbits as prograde), but many studies have found that retrograde orbits are generally more stable than prograde orbits (e.g., Harrington 1972; Mardling & Aarseth 2001; Morais & Giuppone 2012). It is possible that scattering is biased towards producing triples in prograde orbits and there remains an excess of prograde orbits after the unstable triples have dissociated.

The inner eccentricity distributions have two compo-

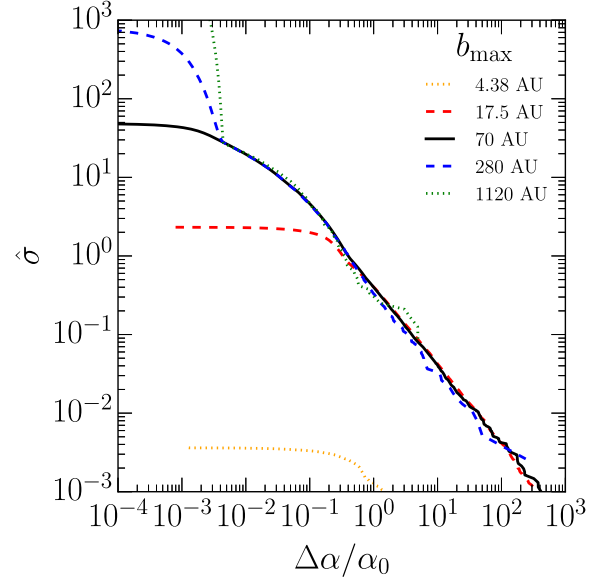


Figure 12. The cumulative cross section for changes to the semi-major axis ratio, α , for a variety of choices of b_{max} . For changes larger than $\Delta \alpha / \alpha_0 \sim 3 \times 10^{-3}$ our calculations using $b_{\text{max}} = 70$ AU are converged. For changes to α smaller than $\sim 3 \times 10^{-3}$ the cross sections diverge with larger b_{max} because α in an isolated triple will vary on this scale over time (see Figure 13). Choices of b_{max} less than 70 AU are not converged down to the limit of $\Delta \alpha / \alpha_0 \sim 3 \times 10^{-3}$, resulting in a smaller asymptotic cross section.

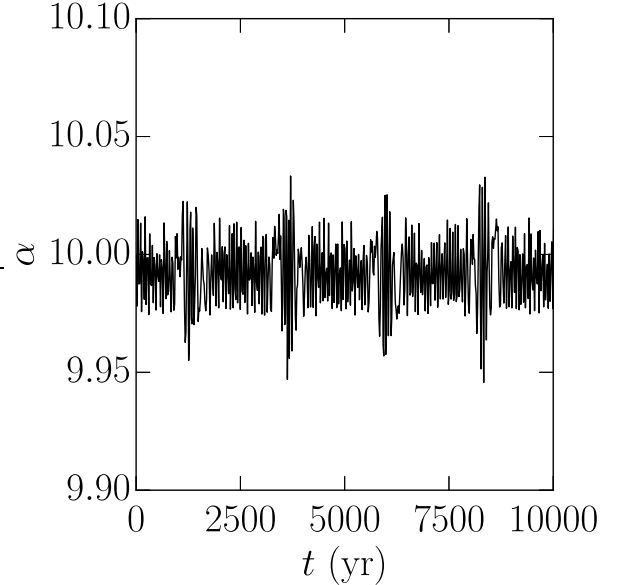


Figure 13. The semi-major axis ratio, α over time for an isolated triple with initial orbital parameters of: $a_{11} = 1$ AU, $a_1 = 10$ AU, $e_{11} = e_1 = 0$, $i = 70^\circ$. The relative variation of α is $\sim 3 \times 10^{-3}$, in agreement with the point of divergence seen in Figure 12.

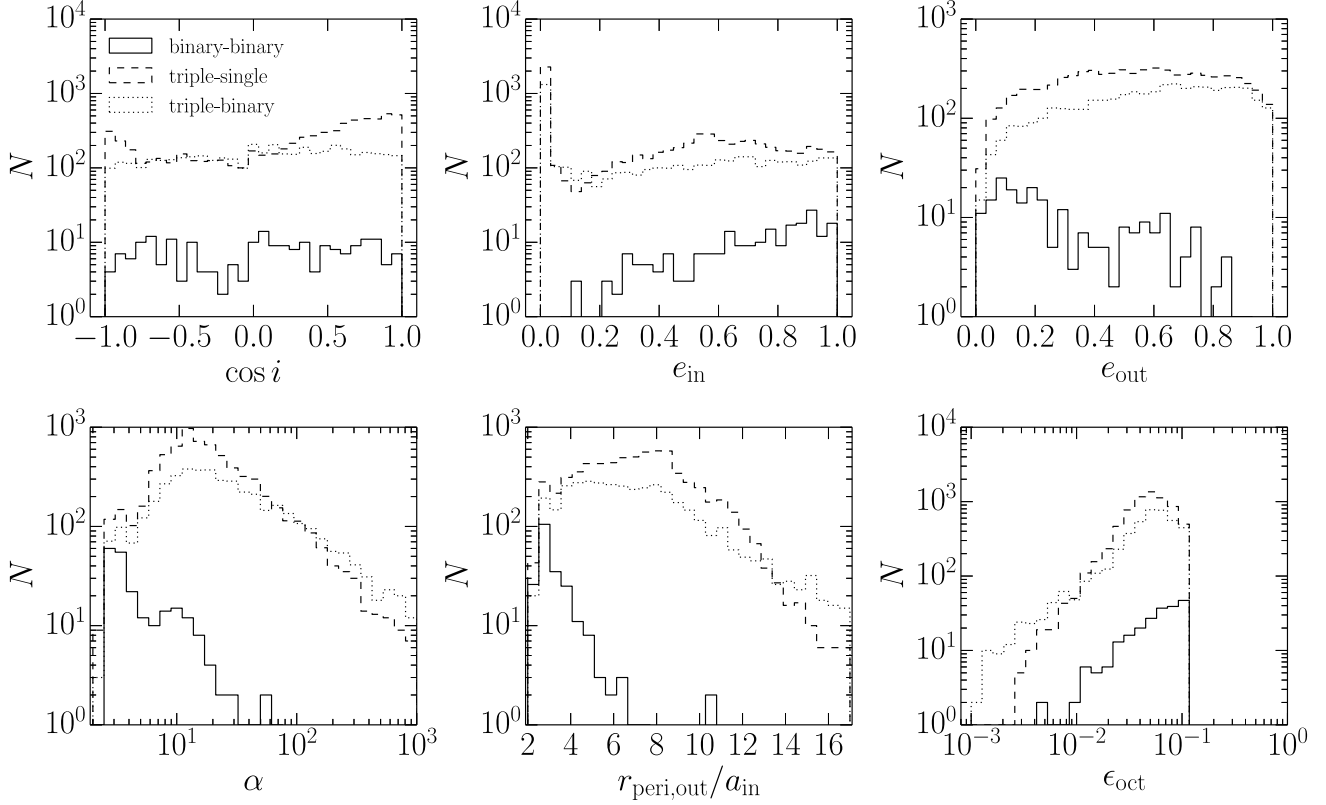


Figure 14. Orbital parameters of dynamically formed triples from binary-binary (solid lines), triple-single (dashed lines), and triple-binary (dotted lines) scattering. The systems consist of $1 M_{\odot}$ stars in circular orbits with a semi-major axis of 1 AU in the case of binary-binary scattering, and $a_{\text{in}} = 1$ AU and $a_{\text{out}} = 10$ AU in the case of triple scattering. We have excluded triples whose final hierarchy is identical to their initial hierarchy. *Upper left:* the inclination distribution for dynamically formed triples. We correct the inclinations for KL oscillations; this panel shows the minimum $\cos i$ that is achieved by KL oscillations. The distribution is approximately uniform in $\cos i$. *Upper middle:* the distribution of inner eccentricities. Both triple-single and triple-binary scattering produce a peak at low eccentricities due to our choice of initial conditions of circular inner orbits. Both also produce a flat distribution of e_{in} whereas binary-binary scattering produces a distribution of e_{in} which is closer to thermal. *Upper right:* The distribution of outer eccentricities. Triples produced from binary-binary scattering are biased towards small e_{out} , but triple scattering produces triples that are slightly biased towards large e_{out} . *Lower left:* the distribution of semi-major axis ratios. *Lower middle:* the distribution of distances at periastris relative to the inner semi-major axis. Dynamically formed triples, particularly those formed from binary-binary scattering, are extremely compact. Most are close to the stability boundary. *Lower right:* the distribution of ϵ_{oct} , a measure of the strength of the octupole order term in the Hamiltonian. Generally, if $\epsilon_{\text{oct}} > 10^{-2}$ the EKM will operate and produce flips for a substantial range of initial inclinations. Although these triples will not exhibit the EKM because all objects are equal mass, dynamically formed triples with unequal masses produce a similar ϵ_{oct} distribution. (See Fig. 16.)

nents, one of which is approximately thermal for high e_{in} . In the case of triple scattering there is also a strong component peaked near $e_{\text{in}} \approx 0$. This is an artifact of the fact that we initialized triples with $e_{\text{in}} = 0$ and many new triples were formed from an exchange between the tertiary and the interloping star. Since these exchange reactions do not strongly affect the inner binary there remains a peak at $e_{\text{in}} \approx 0$.

It is clear from this orbital parameter distribution that a significant fraction of dynamically formed triples undergo strong KL oscillations. The period of these oscillations, t_{KL} , for equal mass systems is given approximately by (Holman et al. 1997; Innanen et al. 1997; Antognini 2015)

$$t_{\text{KL}} = \frac{8}{15\pi} \frac{P_{\text{out}}^2}{P_{\text{in}}} (1 - e_{\text{out}}^2)^{3/2}. \quad (29)$$

Although our calculations are unitless, if we fix the initial semi-major axes of the binaries to 1 AU in the case

of binary-binary scattering and in the case of triple scattering we fix the initial semi-major axis of the inner binary to 1 AU and set all masses to $1 M_{\odot}$ we can calculate the resulting distribution of t_{KL} in years. This distribution is presented in Fig. 15. There are two interesting features: the first is that they are fairly narrow; the vast majority of dynamically formed triples span only one decade in t_{KL} . The second is that t_{KL} is comparable to the initial dynamical timescale of the systems. In the case of binary-binary scattering, the initial periods of the binaries are 0.7 yr and the KL timescales are peaked at approximately 3 yr. Likewise in the case of triple scattering the outer period is 18 yr and the KL timescales have a peak at around 20–30 yr. In the case of triple-single scattering there is an additional peak at even shorter timescales. Such short KL timescales are a consequence of two facts: (1) dynamically formed triples are

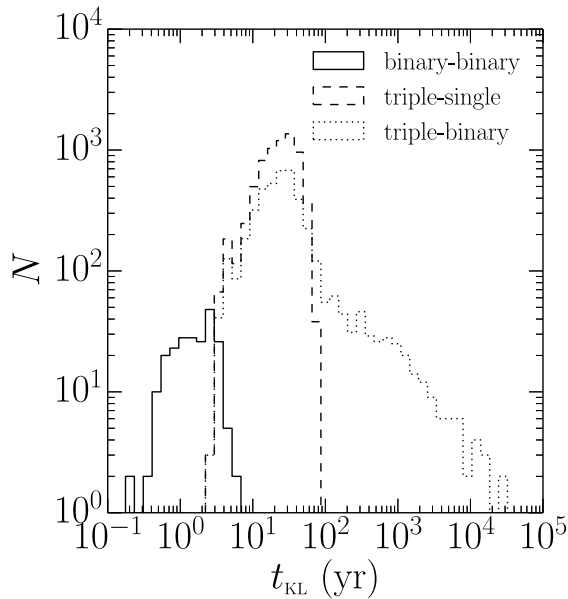


Figure 15. The distribution of the timescale of KL oscillations of dynamically formed triples in a set of model experiments. In the case of binary-binary scattering the initial semi-major axes were set to 1 AU, and in the case of triple scattering we set $a_{\text{in}} = 1$ AU and $a_{\text{out}} = 10$ AU. The masses are all $1 M_{\odot}$. Triple scattering generally produces larger triples and hence longer KL timescales because there is a larger scale in the problem, namely a_{out} . The distributions of t_{KL} do not extend much beyond a decade, except in the case of triple-binary scattering which has a longer tail towards large t_{KL} .

extremely compact, and (2) at the critical velocity triples are more easily formed by hardening binaries than by softening them, thereby leading to smaller semi-major axes and shorter periods.

5.3 Population study

The above analysis reveals that triples produced from our model scattering experiments are extremely compact. It is possible that this result is an artifact from the fact that in binary-binary scattering we scattered binaries with equal semi-major axes and in triple scattering we scattered relatively compact triples. Binary and triple systems in the Galaxy span many decades of semi-major axis, so the components of typical scattering events will not be of comparable scales.

To examine the distribution of orbital parameters of triples produced from a more realistic population of binary and triple systems in the Galaxy we run 10^6 apiece of binary-binary, triple-single, and triple-binary scattering experiments. In each experiment we draw a primary mass from the IMF provided by Maschberger (2013) which is an analytic approximation to the IMFs found by Kroupa (2001) and Chabrier (2003). We then draw secondary and, if applicable, tertiary masses from a uniform distribution bounded by $0.08 M_{\odot}$ and the primary mass. We next draw semi-major axes from a distribution uniform in $\ln a$ from 0.01 to 10^5 AU. In the case of a triple, we draw two semi-major axes and take the smaller to be the semi-major axis of the inner

binary. We then draw eccentricities from a uniform distribution (e.g., Raghavan et al. 2010; Duchêne & Kraus 2013). Lastly we determine the stability of the triple by applying the Mardling stability criterion (equation 14). If the triple is unstable we throw out the entire experiment and resample all parameters. We set the incoming velocity to 40 km s^{-1} , which is approximately the velocity dispersion of older stars in the thin disk (Edvardsson et al. 1993; Dehnen & Binney 1998; Binney & Merrifield 1998). Because we are only interested in the orbital parameters here, and not the cross sections for collisions, we assume all stars to be point masses.

The distribution of orbital parameters of new triples is shown in Fig. 16. Instead of ϵ_{oct} (equation 28) we calculate $\epsilon_{\text{oct},M}$, defined to be (Naoz et al. 2013)

$$\epsilon_{\text{oct},M} = \left(\frac{m_{111} - m_{112}}{m_{111} + m_{112}} \right) \epsilon_{\text{oct}}, \quad (30)$$

where m_{111} and m_{112} are the masses of the two components of the inner binary. This term accounts for the fact that the octupole term in the Hamiltonian has a mass term which vanishes in the case of an equal mass inner binary. Thus, $\epsilon_{\text{oct},M}$ indicates the strength of eccentric KL oscillations. We estimate the timescale for eccentric KL oscillations (i.e., the time between orbital flips) to be (Antognini 2015)

$$t_{\text{EKM}} = \frac{128\sqrt{10}}{15\pi\sqrt{\epsilon_{\text{oct},M}}} t_{\text{KL}}. \quad (31)$$

These results indicate that dynamically formed triples in the field are, as in our model system, extremely compact. The peak of the $\epsilon_{\text{oct},M}$ distribution is broader than the ϵ_{oct} distribution, but centered on $\sim 10^{-2}$, indicating that the vast majority of dynamically formed triples at high inclination undergo strong eccentric KL oscillations. We additionally show the KL timescales and eccentric KL mechanism (EKM) timescales for these triples in Fig. 17. Despite the wide range of orbital periods in the initial systems (with outer periods up to $\sim 10^7$ yr), the KL timescales are all quite short. Nearly all of them are less than 1000 yr. This is due to two facts: (1) the dynamically formed triples are all extremely compact, and so don't have KL timescales much longer than the outer orbital period; and (2) above periods of ~ 1000 yr the binaries become soft and so the cross section for triple formation drops dramatically (see Fig. 8). Furthermore, because $\epsilon_{\text{oct},M}$ is so large, the EKM timescales are generally not substantially larger than the KL time.

6 DISCUSSION

Here we apply our results on binary-binary, triple-single and triple-binary scattering in four contexts. In Section 6.1 we compare the production rate of WD-WD binaries with highly inclined tertiaries via scattering to the SN Ia rate. In Section 6.2 we estimate the number of planets in multiple systems ejected due to scattering and compare to the estimated number of free-floating planets. We then refine our previous calculations by modeling stars with non-zero radii to estimate the rate of stellar collisions in Section 6.3. Finally, in Section 6.4 we address the question of how long KL oscillations persist for triple systems in globular clusters and in the field until they are disrupted by scattering events.

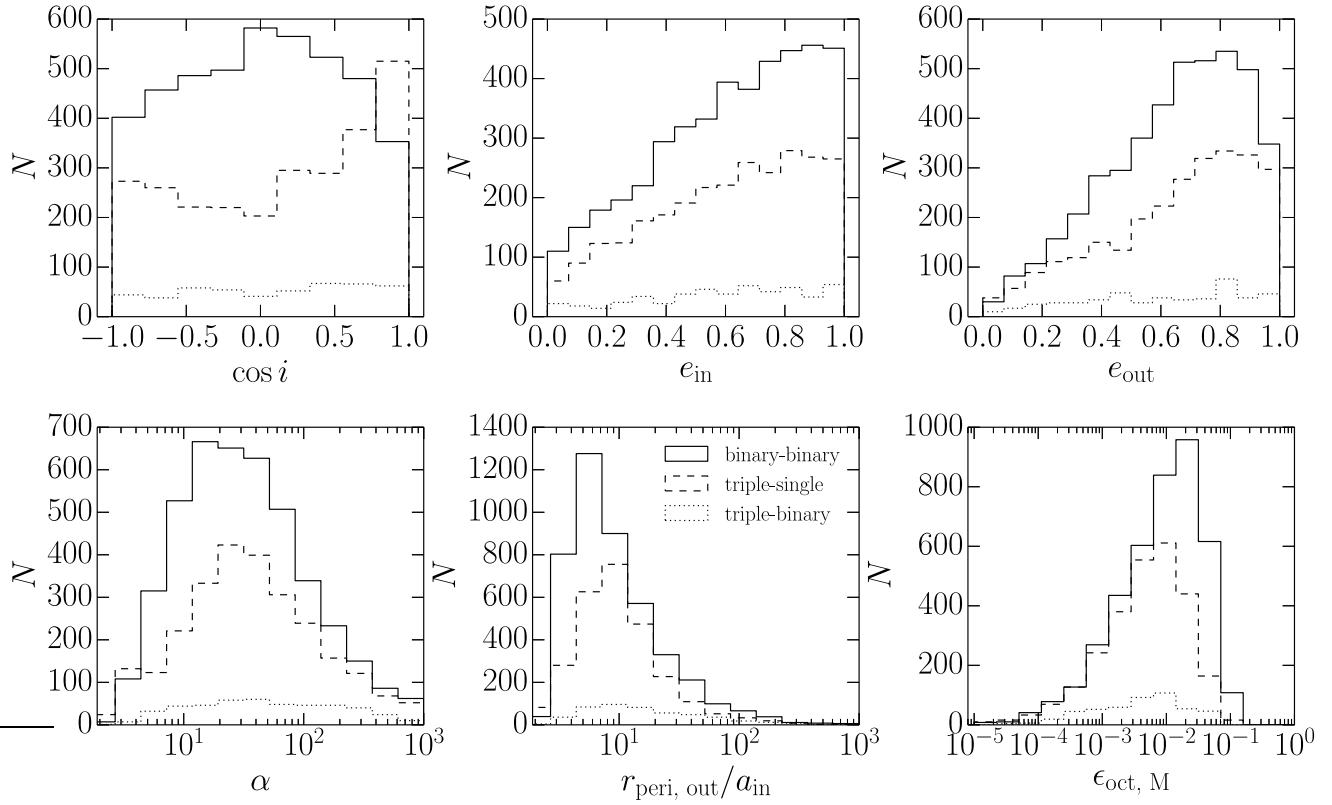


Figure 16. Orbital parameters of new triples resulting from scattering experiments in our population study (Section 5.3). The panels are as in Fig. 14, except for the bottom right panel, where we have used $\epsilon_{\text{oct, M}}$ instead of ϵ_{oct} (see equation 30). As in the model case, triples formed from scattering are extremely compact and have large ϵ_{oct} .

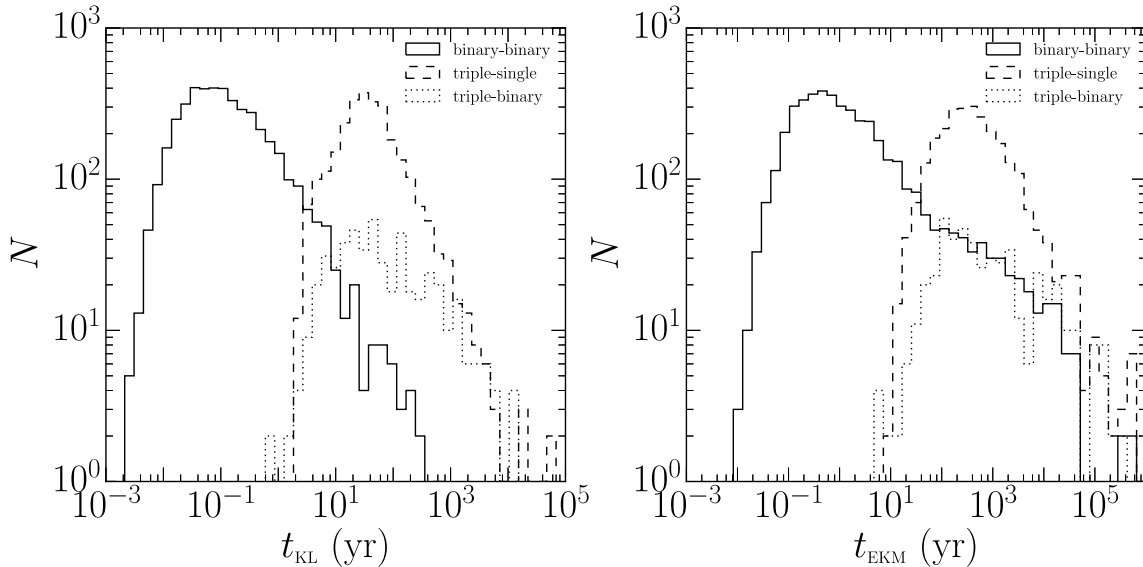


Figure 17. Distribution of the timescales of KL oscillations (left panel) and the eccentric KL mechanism (right panel) in dynamically formed triples in our population study (Section 5.3). Dynamically formed triples have very short KL timescales, with nearly all KL timescales being less than 1000 yr. This is a consequence of the fact that the triples formed are compact and very wide systems are soft, and therefore have low interaction cross sections. Because the triples are so compact the timescale for the eccentric KL mechanism is also very short, nearly always less than 10^5 yr.

6.1 Application to Type Ia Supernovae

The progenitor systems of SNe Ia are currently unknown. The two most viable models are the single degenerate model, in which a WD accretes mass from a main sequence or giant star (Whelan & Iben 1973; Nomoto 1982), and the double degenerate model, in which two WDs merge (Iben & Tutukov 1984; Webbink 1984). In the past several years the double degenerate model has received much observational support (Bloom et al. 2012; Schaefer & Pagnotta 2012; Edwards et al. 2012; González Hernández et al. 2012; Maoz et al. 2014; Shappee et al. 2013), but population synthesis models demonstrate that while it may be possible to match the rate of sub-Chandrasekhar mass WD-WD mergers to the SN Ia rate (Ruiter et al. 2009, 2011; Maoz et al. 2012), hydrodynamical simulations suggest that a large fraction of these mergers may not produce SNe Ia (Nomoto et al. 1997; Maoz & Mannucci 2012; Maoz et al. 2014).

Thompson (2011) provided the first analysis of WD-WD mergers in triple systems and showed that the perturbative influence of the tertiary can decrease the merger time by several orders of magnitude (Miller & Hamilton 2002; Blaes et al. 2002). Thompson (2011) argued that most SNe Ia may occur in triple systems due to the relatively large triple fraction and the larger fraction of triple systems that merge rapidly relative to isolated WD-WD binaries. Moreover, Thompson (2011) speculated that some of these mergers may result in a collision. Katz & Dong (2012) first showed that clean, head-on collisions of two WDs are possible in triple systems using direct N-body calculations and claimed that $\sim 5\%$ of WD-WD binaries with tertiaries produce a direct collision as a result of non-secular dynamics. The triple scenario for SNe Ia is attractive because collisions potentially soften the requirement that the merger mass exceed the Chandrasekhar mass (Rosswog et al. 2009; Raskin et al. 2010; Kushnir et al. 2013). Tertiaries might also hide WD-WD progenitor systems (Thompson 2011). Since the rate of sub-Chandrasekhar mass mergers is comparable to the SN Ia rate (van Kerkwijk et al. 2010; Maoz & Mannucci 2012; Maoz et al. 2012, 2014), this model may solve several problems with the double degenerate model.

The triple scenario has an important obstacle, however. The same KL mechanism that drives the WD-WD binaries to rapidly merge or collide would drive the stars to tidal contact or merger on the main sequence. The main sequence stars would then have either tidally circularized at a few stellar radii or have undergone common envelope evolution. In both cases, the semi-major axis ratio between the inner binary and tertiary would likely increase significantly, rendering the KL mechanism potentially ineffective by the time the stars evolved into WDs. Furthermore, mass loss from one of the stars generally exacerbates this problem by decreasing the mass ratio of the inner binary and triggering the eccentric KL mechanism (Shappee & Thompson 2013). The eccentric KL mechanism can drive the inner binary to much higher eccentricities (Lithwick & Naoz 2011; Katz et al. 2011); thus, even stars that had escaped tidal circularization on the main sequence may be brought into tidal contact after the primary evolves into a WD. While this may be an important source of single degenerate systems, the resulting double degenerate system when the smaller mass

star evolves into a WD may be too wide to merge within a Hubble time. It is, however, possible that some fraction of these systems might evolve into tight WD-WD binaries during common envelope evolution, though it is currently very difficult to make estimates of this fraction (Ivanova et al. 2013).

Naïvely, for the triple scenario to work, it must be possible for a binary to begin its life in a system that does not undergo KL oscillations and then efficiently change into a system that undergoes KL oscillations after evolving into a WD-WD binary. Scattering is a candidate by which this can occur. Although a detailed, comprehensive calculation of the rate is left for future work, we can present an estimate to determine if scattering is a viable channel for the production of high inclination triples. In this estimate we consider three environments: the field, open clusters and globular clusters. We study the field and open clusters separately because the SN Ia delay time distribution is often decomposed into two separate parts: a prompt component which explodes within a few hundred Myr of star formation, and a delayed component which explodes a Gyr or more after star formation (e.g., Scannapieco & Bildsten 2005; Mannucci et al. 2006; Maoz & Badenes 2010). Since the KL timescale is much shorter than the scattering timescale (see Section 6.4), any KL-induced collisions may occur rapidly after the scattering event (e.g., figure 1 of Katz & Dong 2012). The maximum lifetime of open clusters is generally only a few hundred Myr (de La Fuente Marcos 1997; Lamers et al. 2005), so it is plausible that scattering events that contribute to the prompt component occur in open clusters and scattering events that contribute to the delayed component occur in the field. However, WD-WD mergers due to KL oscillations do not necessarily occur instantaneously. Particularly in the case of gravitational wave driven mergers, KL oscillations can take more than a Gyr to drive the WD-WD binary to merger (Thompson 2011). It is therefore possible that scattering events in open clusters could produce SN Ia progenitors which eventually contribute to the delayed component of the SN Ia delay time distribution rather than the prompt component.

We additionally consider scattering in globular clusters. The SN Ia rate in globular clusters is poorly constrained. Based on a lack of detections of SNe Ia in globular clusters, Voss & Nelemans (2012) placed an upper limit on the globular cluster SN Ia rate, but this limit was larger than the Galactic SN Ia rate by a factor of 50. Graham et al. (2015) found one hostless SN Ia which they claimed was likely to be in a globular cluster. Based on this detection they estimated that the SN Ia rate might be enhanced in globular clusters by a factor of ~ 25 .

The Galactic SN Ia rate is $\Gamma_{\text{Ia}} \sim 5 \times 10^{-3} \text{ yr}^{-1}$ (Maoz & Mannucci 2012). If scattering in the field is the primary channel to form high-inclination triple SN Ia progenitors, then the rate at which scattering events produce high-inclination triples must be at least as large as the SN Ia rate. The rate of dynamical formation of new triples may be written

$$\Gamma_{\text{new triple}} = Nn\sigma v, \quad (32)$$

where N is the total number of binaries in the case of binary-binary scattering or the total number of triples in the case of triple scattering, n is the number density of stars, and σ

is the cross section to produce a new triple. If we consider triples or binaries in a small range of semi-major axes, da , then the differential rate is

$$d\Gamma(a) = \frac{dN}{da} n v \sigma(a) da. \quad (33)$$

For our calculation we assume Öpik's law (Öpik 1924),

$$\frac{dN}{da} = \frac{N_0}{a}, \quad (34)$$

where N_0 is a normalization constant set by the total number of binaries or triples, N :

$$N_0 = N \left[\ln \left(\frac{a_{\max}}{a_{\min}} \right) \right]^{-1}. \quad (35)$$

Although a wide log-normal distribution is more accurate (e.g., Duquennoy & Mayor 1991), the flat distribution is simpler to work with analytically and provides an upper limit on the number of systems at the widest semi-major axes.

The cross section for collision can be written in terms of $\hat{\sigma}$ by noting that

$$\sigma(a) = \pi a^2 \hat{\sigma}(\hat{v}). \quad (36)$$

We found in Section 4.2 that the normalized cross section for new triple formation from exchange is proportional to \hat{v}^{-2} for $\hat{v} \ll 1$ and is proportional to \hat{v}^{-6} for $\hat{v} \gg 1$. We may therefore write the cross section as

$$\sigma = \pi a^2 \hat{\sigma}_0 \frac{v_{\text{crit}}^2}{v^2} = \frac{\pi a \hat{\sigma}_0 \eta^2}{v^2}, \quad \hat{v} < 1 \quad (37)$$

and

$$\sigma = \pi a^2 \hat{\sigma}_0 \frac{v_{\text{crit}}^6}{v^6} = \frac{\pi \hat{\sigma}_0 \eta^6}{a v^6}, \quad \hat{v} > 1 \quad (38)$$

where $\hat{\sigma}_0$ is the normalized cross section for high-inclination triple formation at the critical velocity and where we have defined η^2 to be

$$\eta^2 \equiv a v_{\text{crit}}^2 \quad (39)$$

so as to separate out the dependence of v_{crit} on a . η is the same for binaries or triples of any size as long as the masses and semi-major axis ratio remain constant (cf. equations 10 and 11). For the triples we are considering (0.6 M_{\odot} and $\alpha = 10$) we have $\eta^2 \sim 10^3$ AU km² s⁻².

We additionally found in Section 4.2 that at very high velocities the cross section for new triple formation from triple-single scattering is dominated by scrambles, which have a \hat{v}^{-2} dependence. This contribution to the overall cross section for new triple formation may be written

$$\sigma = \pi a^2 \hat{\sigma}_{0,\text{sc.}} \frac{v_{\text{crit}}^2}{v^2} = \frac{\pi a \hat{\sigma}_{0,\text{sc.}} \eta^2}{v^2}, \quad (40)$$

where $\hat{\sigma}_{0,\text{sc.}}$ is the normalized cross section for scrambles at the critical velocity.

Substituting equations (34), (36), (37), and (38) into equation (33) and integrating with respect to a , we find that for binary-binary scattering

$$\Gamma_{a < a_{\text{crit}}} = \frac{\pi N_0 n \hat{\sigma}_0 \eta^2}{v} (a_{\text{crit}} - a_{\min}), \quad (41)$$

and

$$\Gamma_{a > a_{\text{crit}}} = \frac{\pi N_0 n \hat{\sigma}_0 \eta^6}{v^5} \left(\frac{1}{a_{\text{crit}}} - \frac{1}{a_{\max}} \right), \quad (42)$$

where we have defined a_{crit} such that the incoming velocity is equal to v_{crit} ,

$$a_{\text{crit}} = \frac{G m_{11} m_{12}}{\mu v^2}. \quad (43)$$

For triple-single scattering $\Gamma_{a < a_{\text{crit}}}$ remains unchanged, but we instead have

$$\Gamma_{a > a_{\text{crit}}} = \frac{\pi N_0 n \eta^2}{v} \left[\hat{\sigma}_0 \left(\frac{\eta}{v} \right)^4 \left(\frac{1}{a_{\text{crit}}} - \frac{1}{a_{\max}} \right) + \hat{\sigma}_{0,\text{sc.}} a_{\max} \right], \quad (44)$$

where we have assumed that $a_{\max} \gg a_{\min}$. We may then combine these to obtain the overall rate of new triple formation, given by

$$\Gamma_{\text{new triple}} = \frac{\pi N_0 n \hat{\sigma}_0 \eta^2}{v} \times \left[(a_{\text{crit}} - a_{\min}) + \left(\frac{\eta^4}{v^4} \right) \left(\frac{1}{a_{\text{crit}}} - \frac{1}{a_{\max}} \right) \right] \quad (45)$$

for binary-binary scattering, and given by

$$\Gamma_{\text{new triple}} = \frac{\pi N_0 n \hat{\sigma}_0 \eta^2}{v} \times \left[(a_{\text{crit}} - a_{\min}) + \left(\frac{\eta^4}{v^4} \right) \left(\frac{1}{a_{\text{crit}}} - \frac{1}{a_{\max}} \right) + \left(\frac{\hat{\sigma}_{0,\text{sc.}}}{\hat{\sigma}_0} \right) a_{\max} \right] \quad (46)$$

for triple-single scattering. In most cases we have $a_{\min} \ll a_{\text{crit}} \ll a_{\max}$, so this may be further simplified to

$$\Gamma_{\text{new triple}} = \frac{\pi N_0 n \hat{\sigma}_0 \eta^2}{v} \left[a_{\text{crit}} + \left(\frac{\eta}{v} \right)^4 \frac{1}{a_{\text{crit}}} \right] \quad (47)$$

for binary-binary scattering, and

$$\Gamma_{\text{new triple}} = \frac{\pi N_0 n \hat{\sigma}_0 \eta^2}{v} \times \left[a_{\text{crit}} + \left(\frac{\eta}{v} \right)^4 \frac{1}{a_{\text{crit}}} + \left(\frac{\hat{\sigma}_{0,\text{sc.}}}{\hat{\sigma}_0} \right) a_{\max} \right] \quad (48)$$

for triple-single scattering. This implies that nearly all binary-binary scattering events which produce new triples occur for systems in which the outer semi-major axis is such that the critical velocity of the outer binary is close to the velocity dispersion of the surrounding stars. By contrast, new triple formation from triple-single scattering events is dominated by scrambles in systems near the maximum semi-major axis.

Using our scattering experiments from Section 3.2.4 we calculate $\hat{\sigma}_0$ for binary-binary scattering by calculating the cross section for outcomes in which a triple is formed with a mutual inclination of $80^\circ < i < 110^\circ$. Although the range of inclinations that will produce WD-WD collisions is dependent on the semi-major axis (larger systems will produce collisions for a narrower range of inclinations), the dependence of the required inclination on the semi-major axis is not known. We simply assume the inclination range of $80^\circ < i < 110^\circ$ found by Katz & Dong (2012) to produce WD-WD collisions to hold for all scales. The cross sections we use should therefore be considered to be accurate only at the order of magnitude level. We find that for binary-binary scattering $\hat{\sigma}_0 = 2 \times 10^{-5}$. For triple scattering we calculate $\hat{\sigma}_0$ in a similar way, but we only select triples which were initialized with inclinations less than the Kozai angle

($i < 39.2^\circ$ or $i > 141.8^\circ$). We find that for triple scattering (both triple-single and triple-binary) $\hat{\sigma}_0 = 2 \times 10^{-3}$. We likewise calculate the cross section for high-inclination new triple formation from scrambles at the critical velocity in a similar way and find $\hat{\sigma}_{0,sc.} = 7 \times 10^{-5}$.

6.1.1 Estimate for the field

To estimate $\Gamma_{\text{new triple}}$ in the field we make the following assumptions: (1) the total number of white dwarfs in the Galaxy is 10^{10} (Napiwotzki 2009); (2) the fraction of white dwarfs in WD-WD binaries is 10 per cent (Holberg 2009); (3) the fraction of WD-WD binaries with tertiary companions is the same as the fraction of stellar binaries with tertiary companions, i.e., 20 per cent (Raghavan et al. 2010); (4) the volume density of stars in the field is $0.09 \text{ M}_\odot \text{ pc}^{-3}$ (Flynn et al. 2006); (5) the mean star mass is 0.36 M_\odot (Maschberger 2013); and (6) the velocity dispersion of stars in the thin disk is 40 km s^{-1} (Edvardsson et al. 1993; Binney & Merrifield 1998, p. 656).

Under these assumptions the total number of WD-WD binaries is $N_{\text{bin}} = 10^9$, the total number of WD-WD binaries with tertiary companions is $N_{\text{trip}} = 2 \times 10^8$, and the number density in the field is $n = 0.25 \text{ pc}^{-3}$. We additionally take $a_{\text{max}} = 10^4 \text{ AU}$ and $a_{\text{min}} = 10^{-2} \text{ AU}$. From equation (35) we then have $N_{0,\text{bin}} = 7 \times 10^7$, and $N_{0,\text{trip}} = 10^7$, where $N_{0,\text{bin}}$ is the normalization for WD-WD binaries and $N_{0,\text{trip}}$ is the normalization for WD-WD binaries with tertiary companions. Using our data from Section 3.2.4 we calculate the normalized cross section for new triple formation to be $\hat{\sigma}_0 = 2 \times 10^{-3}$ at the critical velocity of the tertiary for triple scattering and $\hat{\sigma}_0 = 2 \times 10^{-5}$ for binary-binary scattering. For systems consisting of solar mass stars with an incoming velocity of 40 km s^{-1} , $a_{\text{crit}} = 0.8 \text{ AU}$. With these numbers, equation (47) gives $\Gamma_{\text{new triple}} \sim 5 \times 10^{-9} \text{ yr}^{-1}$ for triple scattering and $\Gamma_{\text{new triple}} \sim 2 \times 10^{-13} \text{ yr}^{-1}$ for binary-binary scattering in the Galaxy. The rates from triple scattering are several orders of magnitude larger than the rates from binary-binary scattering because the rate from triple scattering is dominated by scrambles at large semi-major axes, which are not a possible outcome of binary-binary scattering. However, rates from both binary-binary and triple scattering are far below Γ_{Ia} . In elliptical galaxies the rates are further depressed relative to the estimate in the Galactic field due to the lower number densities and higher velocity dispersions (and hence lower a_{crit}).

6.1.2 Estimate for open clusters

To estimate $\Gamma_{\text{new triple}}$ for open clusters we make the following assumptions: (1) the typical number density of an open cluster is 10 pc^{-3} (Piskunov et al. 2007); (2) the typical velocity dispersion of an open cluster is 0.3 km s^{-1} ; (3) the binary fraction is 50 per cent and the triple fraction is 10 per cent (Raghavan et al. 2010); (4) the total number of open clusters in the Galaxy is 10^5 (Piskunov et al. 2006); and (5) the typical system is in an open cluster with 300 members (Porrás et al. 2003).

Under these assumptions the total number of triples in open clusters is $\sim 3 \times 10^6$ and the total number of binaries in open clusters is $\sim 2 \times 10^7$. From equation (35) we have

$N_{0,\text{bin}} = 10^6$ and $N_{0,\text{trip}} = 2 \times 10^5$. Note that with our assumed velocity dispersion we have $a_{\text{crit}} \sim 10^4 \text{ AU}$, which is comparable to the semi-major axes of the widest binaries observed. Thus in an open cluster environment we are in the low-velocity regime even for the widest systems. Since scrambles are a dominant channel to produce high inclination triples only at very high velocities, the contribution of scrambles can be neglected in open clusters.

With these numbers, equation (47) gives $\Gamma_{\text{new triple}} \sim 2 \times 10^{-5} \text{ yr}^{-1}$ for triple scattering and $\Gamma_{\text{new triple}} \sim 5 \times 10^{-4} \text{ yr}^{-1}$ for binary scattering in all open clusters in the Galaxy. Thus, even in open cluster environments the new triple formation rate is below the SN Ia rate. These estimates suggest that it is difficult for scattering to produce high-inclination triples at a rate consistent with the SN Ia rate. Moreover, the estimated rate is dominated by scattering events near a_{crit} , which is $\sim 10^4 \text{ AU}$. These separations are only smaller than the typical separations between stars in the open cluster by a factor of a few, so our implicit assumption that each scattering event proceeds in dynamical isolation is likely unwarranted at the largest semi-major axes (see Section 6.1.4).

6.1.3 Estimate for globular clusters

To estimate $\Gamma_{\text{new triple}}$ for globular clusters we make the following assumptions: (1) the typical mass of a globular cluster is $2 \times 10^5 \text{ M}_\odot$ (Harris 1996); (2) the typical half-mass radius is 3 pc (Harris 1996); (3) there are 150 globular clusters in the Galaxy (Harris 1996); (4) 0.7 per cent of the systems in a globular cluster are WD-WD binaries (Shara & Hurley 2002); (5) the triple fraction relative to the binary fraction is the same as the field, i.e., 0.2 (Raghavan et al. 2010);⁵ and (6) the typical velocity dispersion of a globular cluster is 6 km s^{-1} (Harris 1996; Binney & Tremaine 2008, p. 31).

Under these assumptions the average number density in the half-mass radius is $\sim 2500 \text{ pc}^{-3}$, and the typical separation between stars is $\sim 10^4 \text{ AU}$. To maintain our assumption of dynamical isolation we therefore take $a_{\text{max}} = 10^3 \text{ AU}$. Given a median star mass of 0.36 M_\odot (Maschberger 2013), the total number of stars within the half-mass radii of all globular clusters is $\sim 4 \times 10^7$, the number of WD-WD binaries is $\sim 3 \times 10^5$, and the total number of WD-WD binaries with tertiaries is $\sim 6 \times 10^4$. This then implies that $N_{0,\text{bin.}} \sim 3 \times 10^6$ and $N_{0,\text{trip.}} \sim 7 \times 10^5$. We furthermore have $a_{\text{crit}} \sim 40 \text{ AU}$.

With these numbers, equation (47) gives $\Gamma_{\text{new triple}} \sim 10^{-7} \text{ yr}^{-1}$ for binary-binary scattering and $\Gamma_{\text{new triple}} \sim 4 \times 10^{-6} \text{ yr}^{-1}$ for triple scattering for all globular clusters in the Galaxy. To compare these rates with the Galactic SN Ia rate, we note that the total mass in globular clusters is $\sim 3 \times 10^7 \text{ M}_\odot$ whereas the total stellar mass in the Galactic disk is $\sim 5 \times 10^{10} \text{ M}_\odot$ (McMillan 2011). Thus the fraction of stellar mass in globular clusters is $\sim 5 \times 10^{-4}$, so the expected SN Ia rate in globular clusters assuming no enhancement is

⁵ In reality the triple fraction in globular clusters will be determined by the dynamical evolution of the cluster, so there is no reason that the triple fraction in globular clusters should be similar to that of the field. However, the triple fraction in globular clusters is poorly constrained, though it is unlikely to be very much higher than that of the field, so we assume here a triple fraction to binary fraction of 0.2 as a rough upper limit.

$\sim 3 \times 10^{-6} \text{ yr}^{-1}$. This is comparable to the scattering rates that we find. Thus, if the SN Ia rate is not enhanced in globular clusters, scattering could be an important channel to form WD-WD binaries with high inclination tertiaries. If, however, the SN Ia rate is enhanced by a factor of ~ 25 as claimed by Graham et al. (2015) scattering would be unlikely to be the primary channel by which to produce SN Ia progenitors in triples.

6.1.4 Summary of rate estimates

Although there are substantial uncertainties and simplifications in the analysis of this subsection, these results imply that if the triple scenario is correct, either scattering of very wide triples in open clusters leads to the formation of high-inclination triple systems or a mechanism other than scattering is responsible for the formation of high-inclination triple systems. It also may be that the full dynamics of open clusters beyond the isolated scattering events we have considered here (such as the dissociation of the cluster) are important for the formation of WD-WD binaries in high inclination triple systems. While we have treated scattering events in open clusters in isolation, this is likely not a good approximation, particularly at the large semi-major axes considered here (Geller & Leigh 2015). It is also possible that triple-binary scattering produces quadruples, which undergo strong KL oscillations over a wider range of parameter space (Pejcha et al. 2013). Scattering in globular clusters is more promising, as the rate of new triple formation can match the Galactic SN Ia rate (after correcting for the fraction of mass in globular clusters). Finally, we note that our calculations of the normalized cross sections were done assuming relatively compact triples (semi-major axis ratios of 10) and binaries of equal size. The distribution of semi-major axis ratios of triples in the Galaxy will certainly be broader than we assumed, so the true normalized cross sections will be different from the cross sections we calculated. Indeed, they will likely be lower due to the fact that scattering is generally more efficient in compact triples—see Section 5.3. These issues should be investigated more fully in a future work.

We conclude that scattering in the field cannot produce WD-WD binaries in high-inclination triples at a rate consistent with the SN Ia rate, but we cannot rule out the possibility that scattering in open clusters and globular clusters leads to high inclination triples at rates consistent with the SN Ia rate.

6.2 Application to free-floating planets

The dynamical effect of interloping stars or binaries on planetary systems has been studied extensively (see Adams 2010 for a review). Malmberg et al. (2007) measured the rate of close encounters between stars in an open cluster environment and found that dynamical processes will alter the population of planetary systems similar to the Solar System. Malmberg & Davies (2009) found that these close encounters can produce eccentric orbits with an eccentricity distribution similar to the observed distribution of eccentricities of very eccentric exoplanets. Malmberg et al. (2011) calculated the long-term effect of distant flybys on planetary systems and showed that ~ 10 per cent of systems are pushed

from a configuration which is stable on timescales of $\sim 10^8$ yr to a configuration which is unstable on these timescales. Most recently, Li & Adams (2015) calculated the cross sections for various outcomes and changes to the orbital parameters from scattering events between a planetary system and a binary star. In this subsection we apply our results to the free-floating planet population.

Microlensing surveys have claimed the existence of a large population of free-floating planets (Zapatero Osorio et al. 2000; Sumi et al. 2011). It is unknown whether these sub-brown dwarf objects form in isolation or if they were ejected from the planetary systems in which they were born. Numerical simulations indicate that it may be difficult for planet-planet scattering to fully account for the observed numbers of free-floating planets (Veras & Raymond 2012). While there is some observational evidence for the isolated formation of sub-brown dwarf objects in the Rosette Nebula (Gahm et al. 2013), it is nevertheless unclear if isolated formation is the dominant channel for the production of free-floating planets.

We here examine the efficiency of planet ionization due to scattering events. We perform three classes of scattering events: (1) a multi-planet system scattering off of a single or binary star system, (2) a circumbinary planetary system (i.e., a P-type orbit) scattering off of a single or binary star system, and (3) a planetary system in a binary (i.e., an S-type orbit) scattering off of a single or binary star system. We furthermore examine planet scattering in both open clusters and in the field. In these experiments the masses of the stars are set to $1 M_{\odot}$ and the planets are set to $0.01 M_{\odot}$. In the triple systems the inner object is given a semi-major axis of 1 AU and the outer object is given a semi-major axis of 20 AU and the orbits are set to be coplanar. (In the case of a multi-planet system we instead set the semi-major axis of the inner planet to 4 AU to encourage planet-planet scattering.) In the case of scattering off of a binary, the incoming binary is given a semi-major axis of 100 AU. For the field the incoming velocity is set to 40 km s^{-1} and for open clusters it is set to 3 km s^{-1} . Our assumed incoming velocity for open clusters is larger in this section than in Sections 6.1 and 6.3 due to the fact that the scattering experiments we perform in this subsection are prohibitively expensive at an incoming velocity of 0.3 km s^{-1} . Consequently we calculate the cross sections at this larger incoming velocity and later scale the results to a lower incoming velocity.

With these initial conditions we then calculate the cross section for planet ionization and present them in Table 6. In all systems in the field the normalized cross section is within an order of magnitude of unity. In open clusters the cross section is enhanced by one to two orders of magnitude because the incoming velocity is smaller by a factor of ~ 10 . Multi-planet–single scattering has the largest normalized cross section due to induced planet-planet scattering. Although this effect is also present in multi-planet–binary scattering, its normalized cross section is much lower simply due to the much larger area of the interloping binary. The physical cross section for planet ionization is slightly larger in multi-planet–binary scattering than multi-planet–single scattering.

Table 6. Cross sections for planet ionization. We include both the normalized cross section, $\hat{\sigma}$, and the physical cross section, σ . Multi-planet systems consist of two planets, circumbinary systems consist of a planet orbiting a binary, and S-type planets consist of a planet orbiting a star in a binary system.

FIELD ENVIRONMENT		
System	$\hat{\sigma}$	σ (AU ²)
Multi-planet–single	6.52 ± 1.14	2608 ± 457
Multi-planet–binary	0.32 ± 0.05	3325 ± 508
Circumbinary–single	3.21 ± 0.08	1285 ± 31
Circumbinary–binary	4.00 ± 0.09	41648 ± 950
S-type planet–single	0.68 ± 0.02	272 ± 7
S-type planet–binary	1.26 ± 0.03	13147 ± 309

OPEN CLUSTER ENVIRONMENT		
System	$\hat{\sigma}$	σ (AU ²)
Multi-planet–single	68.73 ± 14.57	27493 ± 5828
Multi-planet–binary	15.57 ± 4.44	161879 ± 46219
Circumbinary–single	53.59 ± 6.69	21436 ± 2675
Circumbinary–binary	15.20 ± 3.51	158082 ± 36466
S-type planet–single	64.43 ± 2.03	25771 ± 811
S-type planet–binary	7.57 ± 0.77	78703 ± 8046

The timescale for planet ionization can be written

$$\begin{aligned}
 t_{\text{scatter}} &= \frac{1}{\pi n \hat{\sigma} a_{\text{out}}^2 v} \\
 &= \frac{1.1 \times 10^{12}}{\hat{\sigma}} \left(\frac{n}{10 \text{ pc}^{-3}} \right)^{-1} \left(\frac{a_{\text{out}}}{20 \text{ AU}} \right)^{-2} \left(\frac{v}{3 \text{ km s}^{-1}} \right)^{-1} \text{ yr}.
 \end{aligned}
 \tag{49}$$

Even for the outcomes with the largest cross sections ($\hat{\sigma} \sim 70$) the ionization timescale for a given system in a cluster is ~ 20 Gyr. We noted above that $\hat{\sigma}$ was calculated for an incoming velocity of 3 km s^{-1} . For a more realistic incoming velocity of 0.3 km s^{-1} , $\hat{\sigma}$ would increase by two orders of magnitude due to gravitational focusing. However, the scattering timescale is also proportional to v^{-1} , so the overall effect of a smaller incoming velocity would be to decrease the ionization timescale by one order of magnitude to ~ 2 Gyr. This implies that planet ionization from scattering with interloping stellar systems is rare in stellar clusters; only ~ 10 per cent of systems with planets on wide orbits would have lost them in a cluster with an age of 200 Myr. In the field, planet ionization occurs even less frequently due to the lower densities and cross sections. Assuming a stellar density of 0.1 pc^{-3} , a typical velocity of 40 km s^{-1} , and a normalized cross section of ~ 6 , the scattering timescale is $\sim 4 \times 10^{12}$ yr. Thus, fewer than 1 per cent of systems with planets on wide orbits would have lost them in the lifetime of the Galaxy. Scattering from interloping systems can therefore produce some free-floating planets, but not at the level claimed by Sumi et al. (2011).

6.3 Stellar collisions during scattering events

Although the distances between stars are typically much larger than their radii, close encounters between stars can result in tidal interactions, mergers, and collisions. Candidates for observed outbursts from collisions or merg-

ers include V838 Mon and V1309 Sco (Bond et al. 2003; Tytenda & Soker 2006; Tytenda et al. 2011; Kochanek et al. 2014). It is still unclear whether they should preferentially occur between stars born in the same system or between stars in different systems (Leigh et al. 2011; Perets & Kratter 2012). If collisions are typically between stars in the same system, then these collisions would be driven either by dynamical instabilities in the primordial system (in which case collisions will occur not long after the protostar reaches the main sequence, if it ever does) or due to KL oscillations. If, however, a substantial fraction of collisions are between stars in different systems, then this necessarily implies that scattering would be an important channel for stellar collisions.

6.3.1 Numerical calculations

Collisions are always a possibility in resonant scattering events because such events are chaotic. We here rerun our model system ($a_{\text{in}} = 1 \text{ AU}$, $a_{\text{out}} = 10 \text{ AU}$ —see Section 3.1) but we now give the stars radii of $1 R_{\odot}$. We do not include the effects of tides. We halt the calculation after a single collision, so multiple collisions are not considered.

To calculate these cross sections we must account for the fact that some fraction of the observed collisions in triple-single and triple-binary scattering are due to KL oscillations and are not induced by scattering. To correct for this effect we run an identical set of triples in isolation for the same length of time and calculate the fraction of triples that collide. This fraction (\sim few per cent) is then subtracted from the observed collision fraction from the scattering experiments before the cross section is calculated. We find that the normalized cross section for collision at the critical velocity is $\hat{\sigma}_0 = 0.109 \pm 0.004$ for binary-binary scattering, $\hat{\sigma}_0 = 0.134 \pm 0.004$ for triple-single scattering, and $\hat{\sigma}_0 = 0.235 \pm 0.007$ for triple-binary scattering.

Because these calculations are all done in the equal mass case, they are biased towards scattering-induced collisions and away from KL-induced collisions because EKM oscillations will be stronger, leading to a larger collision fraction for triples in isolation. It is also plausible that at more extreme mass ratios ionizations will be a more common outcome (see Section 3.2.3), leading to fewer scattering-induced collisions. This implies that the collision cross sections derived above are likely upper limits. We do not calculate the velocity dependence of the collision cross sections, however, so we cannot rigorously assert that these cross sections are upper limits.

6.3.2 Rate calculation

We show in Appendix A that the velocity dependence of the collision cross section for three-body interactions scales as \hat{v}^{-2} for $\hat{v} \ll 1$ and \hat{v}^{-6} for $\hat{v} \gg 1$ so long as \hat{v} is much less than the escape speed of the stars. Collisions are therefore an exchange-like process. Because of this, the rate of stellar collisions from scattering may be estimated in the same way as the new triple formation rate was estimated in Section 6.1. We here follow the same analysis to estimate the rate of collisions due to scattering with one modification. Because we hold the stellar radii fixed, the ratio (R/a) varies

as we vary a . Fregeau et al. (2004) found that the collision cross section scales linearly with the ratio (R/a) for binary-binary scattering, so we incorporate this factor into the rate calculation:

$$\sigma = \pi a^2 \hat{\sigma}_0 \frac{v_{\text{crit}}^2}{v^2} \left(\frac{a_0}{a} \right) = \frac{\pi a_0 \hat{\sigma}_0 \eta^2}{v^2}, \quad \hat{v} < 1, \quad (50)$$

and

$$\sigma = \pi a^2 \hat{\sigma}_0 \frac{v_{\text{crit}}^6}{v^6} \left(\frac{a_0}{a} \right) = \frac{\pi a_0 \hat{\sigma}_0 \eta^6}{a^2 v^6}, \quad \hat{v} > 1, \quad (51)$$

where a_0 is the outer semi-major axis at which $\hat{\sigma}_0$ was calculated of 10 AU and η is defined as in Section 6.1. Note that we assume here that the collision cross sections for triple-single and triple-binary scattering carry the same (R/a) dependence as binary-binary scattering. Proceeding to integrate equation (33) as we did before, we find

$$\Gamma_{\text{collision}} = \frac{\pi N_0 n \hat{\sigma}_0 \eta^2 a_0}{v} \left[\ln \left(\frac{a_{\text{crit}}}{a_{\text{min}}} \right) + \frac{1}{2} \left(\frac{\eta^4}{v^4} \right) \frac{1}{a_{\text{crit}}^2} \right], \quad (52)$$

where, as in equation (47), we have neglected a_{max} .

We now evaluate $\Gamma_{\text{collision}}$ for the field, open cluster environments, and globular cluster environments using the same assumptions as we did in Section 6.1. We additionally assume that the mass of the Galactic disk is $5 \times 10^{10} M_{\odot}$ (Dehnen & Binney 1998). Given a mean stellar mass of $0.36 M_{\odot}$ (Maschberger 2013), this implies that the total number of systems in the Galactic disk is 1.4×10^{11} . Making use of our assumption that 10 per cent of systems are triples (Raghavan et al. 2010), this implies that the total number of triples is 1.4×10^{10} , and the normalization constant of equation (35) is $N_0 = 10^9$ for the field. We assume the same normalization constant for open clusters as we did in Section 6.1 of $N_0 = 2 \times 10^5$. Furthermore, assuming a typical stellar mass of $0.36 M_{\odot}$ we find $\eta^2 \sim 850 \text{ AU km}^2 \text{ s}^{-2}$. With these numbers we estimate $\Gamma_{\text{collision}} \sim 2 \times 10^{-6} \text{ yr}^{-1}$ in the field, $\sim 9 \times 10^{-6} \text{ yr}^{-1}$ in open cluster environments. For globular clusters we assume that the binary fraction is 3 per cent (Milone et al. 2012) and the ratio of the triple fraction to the binary fraction is 0.2 as it is in the field. This implies a normalization constant for globular clusters of $N_0 = 3 \times 10^6$ and a collision rate of $\sim 8 \times 10^{-4} \text{ yr}^{-1}$ in globular cluster environments. The ratio between the estimated rate in the open clusters and the field is much smaller here than in the case of our SN Ia rate estimate because a_{crit} is much larger in open clusters, leading to smaller values of (R/a), and hence smaller collision cross sections.

These rates are much smaller than the observed rate of stellar mergers in the Galaxy of $\sim 0.5 \text{ yr}^{-1}$ (Kochanek et al. 2014). This implies that scattering is a relatively minor contributor to the stellar merger rate. Of course, since ~ 10 per cent of all triples are formed at inclinations $|\cos i| \leq 0.1$, many of these systems will undergo merger events, and will therefore likely be a much more important contributor to the stellar merger rate. We also note that as in Section 6.1, our assumption of dynamical isolation is likely invalid in an open cluster environment. We save a treatment of the full dynamics of open clusters for a future work.

6.4 How long do high inclination triples survive?

Although KL oscillations can drive interesting behavior in a diverse set of systems in isolation, real systems are not isolated. Perturbations to the gravitational potential of a hierarchical triple generally suppress the KL resonance. While several of these effects have already been studied in detail (e.g., relativistic precession), scattering has not.

Scattering will suppress KL oscillations on the timescale of an interaction in which the triple is scattered from a high-inclination state to a low-inclination state or some other configuration in which KL oscillations are not present (e.g., two binaries). Moreover, if this timescale is much shorter than the timescale of KL oscillations themselves, KL oscillations will not occur at all.

To calculate the lifetime of high inclination triples we performed a suite of scattering experiments over a range of outer semi-major axes with a semi-major axis ratio of 10. We performed experiments in two conditions: the field, for which we take the incoming velocity to be 40 km s^{-1} ; and globular clusters, for which we take the incoming velocity to be 6 km s^{-1} . The scattering timescale is calculated from the cross section for the triple to either disrupt or change its inclination from the range $80^\circ < i < 110^\circ$ (see Section 6.1) to less than the Kozai angle ($i < 39^\circ$ or $i > 141^\circ$). We take the number density of stars to be 0.25 pc^{-3} in the field and 10^4 pc^{-3} in globular clusters.

The scattering timescales for triple-single and triple-binary scattering, along with t_{KL} is shown in Fig. 18. The scattering timescale, t_{scat} , is proportional to a^{-1} because, for fixed incoming velocity, $\sigma/a^2 \propto v_{\text{crit}}^2$ (Hut & Bahcall 1983) and $v_{\text{crit}}^2 \propto a$.

In the field the density of stars is so low that high inclination triples persist for a Hubble time except for the very widest triples ($a_{\text{out}} \gtrsim 10^5 \text{ AU}$). Globular clusters are dense enough, however, that high-inclination triples wider than \sim few AU will be disrupted in a Hubble time. But even in globular clusters, triples as wide as 1000 AU will undergo many KL oscillations before disruption by scattering. This analysis ignores the cumulative effect of many perturbations to the angular momentum of the outer binary, however. At velocities much larger than the critical velocity, perturbations to the angular momentum of a binary become much larger than perturbations to its energy. Very distant passages cause the angular momentum of wide binaries to undergo a random walk and can generally lead to extremely large eccentricities before disruption occurs (Kaib & Raymond 2014). In the case of a triple with a wide outer binary, these perturbations can drive the triple to instability in less time than it would take the triple to disrupt due to scattering alone. Moreover, if the cumulative effect of many distant passages can be modeled as a global tidal field, the outer binary of a wide triple will undergo eccentricity oscillations similar to KL oscillations (Katz & Dong 2011). Since the cumulative effect of multiple distant perturbations can have a substantial impact on the orbital parameters of a triple system on long timescales, particularly in dense environments like globular clusters, these long-term effects should be more fully investigated.

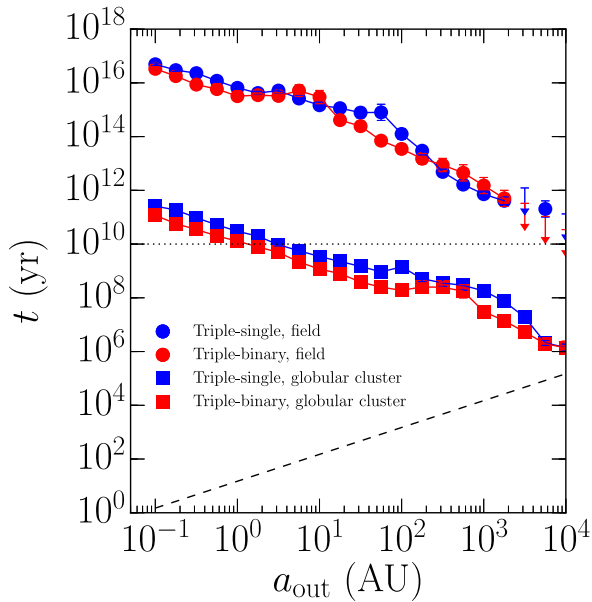


Figure 18. The lifetime of high-inclination triple systems in globular clusters and in the field. Triple systems in the field persist for a Hubble time out to widths of 10^5 AU and triple systems in globular clusters persist for a Hubble time (black dotted line) out to widths of a few AU. We also include the KL timescale (black dashed line). For all but the widest triples in globular clusters the scattering time is much longer than t_{KL} . All but the very widest triples in globular clusters therefore undergo many KL oscillations before disruption by scattering. The scattering timescale is proportional to the inverse of the outer semi-major axis (blue dotted line).

7 CONCLUSIONS

We have explored the properties of binary-binary, triple-single, and triple-binary scattering events in a wide variety of contexts using over 400 million numerical scattering experiments. We have calculated the cross sections for the outcomes of these scattering events in several model systems and grouped these outcomes into a small number of outcome classes (Tables 1, 2, 3, and 4). These outcome classes can, in turn, be broadly grouped into “exchange-like” and “ionization-like” outcomes based on their velocity dependence in analogy to binary-single scattering. Ionization-like outcomes exhibit a \hat{v}^{-2} dependence at large \hat{v} and exchange-like outcomes exhibit a steeper velocity dependence at large \hat{v} (often \hat{v}^{-6} , but sometimes \hat{v}^{-4} —see Fig. 6). The statistical uncertainties on these cross sections are on the order of a few per cent or less. The systematic uncertainty is comparable, but only serves to increase the cross sections of ionization-like outcomes.

We find that the cross section for new triple formation is “exchange-like,” and at the critical velocity the normalized cross section for new triple formation is $\hat{\sigma}_0 = 0.1$ for both triple-single and triple-binary scattering, and $\hat{\sigma}_0 = 0.02$ for binary-binary scattering. At high velocities the new triple cross section has a \hat{v}^{-6} dependence for binary-binary scattering. For triple-single scattering, the new triple cross section also has a \hat{v}^{-6} dependence for velocities slightly in excess of the critical velocity, but at high velocities, scrambles, which have a \hat{v}^{-2} dependence, are the dominant channel to form

new triples. Similarly, the cross section for quadruple formation from triple-binary scattering is an exchange-like process with a \hat{v}^{-6} dependence at high velocity. These results imply that quadruple formation and triple formation in environments dominated by binary-binary scattering are efficient only if the velocity is below the critical velocity (i.e., in cluster environments). In high velocity environments, triple-single scattering is the dominant channel to produce new triples.

We provide analytic fits for the velocity dependence of the ionization cross sections in binary-single, binary-binary, and triple-single scattering (equations 20 and 22). We also provide analytic fits for the velocity dependence of the new triple cross sections in binary-binary and triple-single scattering (equations 25 and 26).

We measure the dependences of the cross sections on various orbital parameters. We find that the dependence of the cross sections on the semi-major axis ratio can be attributed entirely to changes in the critical velocities of the various components, at least as long as the semi-major axis ratio is greater than ~ 10 (Fig. 3).

We find that there is no eccentricity dependence on the cross sections, except insofar as triples with more eccentric tertiaries come closer to the boundary of stability (Fig. 4). Weaker perturbations to the eccentricity of the tertiary can therefore cause the triple to destabilize, leading to a modest increase in the ionization cross section for large outer eccentricities. This increase is well modeled using our fit to the cross section for changes to the outer eccentricity in flyby outcomes. We also studied the mass dependence of the cross sections and find that in general cross sections increase for ionization-like outcomes in binary-binary and triple-binary scattering as the mass of a single star tends toward infinity (Fig. 5). In triple-single scattering the cross sections for all outcomes decrease in the high mass limit because the interloping system cannot be disrupted.

Almost all scattering events are simple flybys which leave the hierarchical structure intact. We calculate the cross section for changes to the orbital parameters after flybys in triple-single and triple-binary scattering events (Fig. 10). We find that changes to the eccentricity of the tertiary are well fit by a Gompertz function (equation 27). The normalized cross section for a large change in the inclination of the triple ($\Delta \cos i \sim 0.5$) is $\hat{\sigma} \sim 0.1$ after correcting for changes to the inclination due to Kozai-Lidov oscillations (panel c of Fig. 10).

We study the properties of triples formed from scattering events and find that dynamically formed triples are extremely compact (Figs. 14 and 16). Indeed, most dynamically formed triples are very close to the stability boundary although longer-term simulations indicate that they are stable for at least hundreds of orbits. Because these triples are so compact, the timescale for Kozai-Lidov oscillations is very short, sometimes just a few times the outer orbital period (Figs. 15 and 17). These triples should therefore exhibit strong non-secular dynamics. We furthermore find that the inclination distribution of dynamically formed triples is approximately uniform in $\cos i$ and the distribution of outer eccentricities is approximately thermal. These results hold both for a model system and for a population study where we model scattering events in the field.

Because many-body gravitational dynamics are ubiqui-

tous in astrophysics, our results have implications in a variety of different contexts. We find that scattering in the field cannot produce high inclination triple systems at a rate consistent with the SN Ia rate, particularly in ellipticals. This result poses problems for the triple scenario for SNe Ia because high inclination triples need to be produced after the stars that eventually comprise the inner binary of the triple evolve into WDs. If this does not occur KL oscillations will drive the inner binary to tidal circularization and will suppress future KL oscillations. We show in Section 6.1 that scattering in open clusters is more efficient and can produce high inclination triples at a rate a factor of ~ 20 below the SN Ia rate. However, it is unlikely that our assumption of dynamical isolation in open clusters is valid, so the formation of high inclination triples may be more efficient than we have estimated when the full dynamics of the cluster are considered. A triple scenario where intermediate mass stars in binaries or triple systems evolve to WDs and then scattering leads to high inclination tertiaries may therefore be an important contributor to the prompt component of the SN Ia delay time distribution. If the time for KL oscillations to drive the WD-WD binary to merger is much longer than the lifetime of the cluster, scattering in open clusters could also contribute to the delayed component of the delay time distribution. We save a complete exploration of scattering in cluster environments and its implications for SNe Ia for a future work.

Scattering can also lead to collisions between stars. We show that the velocity dependence for collisions in binary-single scattering due to three-body interactions is exchange-like with a high-velocity dependence of \hat{v}^{-6} . We estimate the rate of stellar collisions in the Galaxy due to triple scattering to be $\sim 2 \times 10^{-6} \text{ yr}^{-1}$. In open cluster environments the estimated collision rate is comparable, $\sim 9 \times 10^{-6} \text{ yr}^{-1}$. In globular cluster environments the estimated collision rate is larger, $\sim 8 \times 10^{-4} \text{ yr}^{-1}$, due principally to the higher number densities and higher velocity dispersion relative to open clusters. However, our assumptions about dynamical isolation are likely not valid in an cluster environments (Geller & Leigh 2015). The collision rate in clusters may therefore be much higher than our naïve analysis suggests.

We additionally apply our results to several different types of planetary systems and find that scattering from external encounters is a negligible contributor to the free-floating planet population compared to planet-planet scattering. However, in dense open clusters nearly 10 per cent of planets on wide (~ 100 AU) orbits will be ionized due to scattering with interloping systems.

We finally examine the stability of KL oscillations to scattering events (Fig. 18). We find that the cross section for the triple to move from a high-inclination to a low-inclination state is small enough that the timescale to scatter out of a regime in which KL oscillations take place is much longer than the Hubble time for systems in the field and all systems with outer semi-major axes \lesssim few AU in globular clusters. Furthermore, in both the field and in globular clusters the KL timescale is much shorter than the scattering timescale. Thus triples with moderate semi-major axis ratios in any environment may be considered sufficiently isolated that at least several KL oscillations will proceed undisturbed.

ACKNOWLEDGMENTS

We thank John Fregeau for releasing FEWBODY under the GNU Public License. JMA thanks Benjamin Shappee and Daniel Fabrycky for useful discussion. JMA thanks Nathan Leigh and Adrian Hamers for a careful read of the manuscript and helpful comments. The authors thank the referee for a timely and helpful report. This paper made use of MATPLOTLIB (Hunter 2007), IPYTHON (Pérez & Granger 2007), and GNU parallel (Tange 2011). This research made use of Astropy, a community-developed core Python package for Astronomy (Astropy Collaboration et al. 2013). This work was supported in part by an allocation of computing time from the Ohio Supercomputer Center. This research was supported by the National Science Foundation under NSF AST Award No. 1313252.

REFERENCES

- Adams F. C., 2010, *ARA&A*, 48, 47
 Antognini J. M., Shappee B. J., Thompson T. A., Amaro-Seoane P., 2014, *MNRAS*, 439, 1079
 Antognini J. M. O., 2015, *MNRAS*, 452, 3610
 Antonini F., Murray N., Mikkola S., 2014, *ApJ*, 781, 45
 Antonini F., Perets H. B., 2012, *ApJ*, 757, 27
 Astropy Collaboration et al., 2013, *A&A*, 558, A33
 Bacon D., Sigurdsson S., Davies M. B., 1996, *MNRAS*, 281, 830
 Binney J., Merrifield M., 1998, *Galactic Astronomy*
 Binney J., Tremaine S., 2008, *Galactic Dynamics: Second Edition*. Princeton University Press
 Blaes O., Lee M. H., Socrates A., 2002, *ApJ*, 578, 775
 Bloom J. S. et al., 2012, *ApJL*, 744, L17
 Bode J. N., Wegg C., 2014, *MNRAS*, 438, 573
 Boekholt T., Portegies Zwart S., 2015, *Computational Astrophysics and Cosmology*, 2, 2
 Bond H. E. et al., 2003, *Nature*, 422, 405
 Chabrier G., 2003, *PASP*, 115, 763
 Chazy J., 1929, *Journal de mathématiques pures et appliquées*, 353
 de La Fuente Marcos R., 1997, *A&A*, 322, 764
 Dehnen W., Binney J. J., 1998, *MNRAS*, 298, 387
 Dong S., Katz B., Socrates A., 2014, *ApJL*, 781, L5
 Duchêne G., Kraus A., 2013, *ARA&A*, 51, 269
 Duquennoy A., Mayor M., 1991, *A&A*, 248, 485
 Edvardsson B., Andersen J., Gustafsson B., Lambert D. L., Nissen P. E., Tomkin J., 1993, *A&A*, 275, 101
 Edwards Z. I., Pagnotta A., Schaefer B. E., 2012, *ApJL*, 747, L19
 Fabrycky D., Tremaine S., 2007, *ApJ*, 669, 1298
 Flynn C., Holmberg J., Portinari L., Fuchs B., Jahreiß H., 2006, *MNRAS*, 372, 1149
 Ford E. B., Kozinsky B., Rasio F. A., 2000, *ApJ*, 535, 385
 Fregeau J. M., Cheung P., Portegies Zwart S. F., Rasio F. A., 2004, *MNRAS*, 352, 1
 Gahm G. F., Persson C. M., Mäkelä M. M., Haikala L. K., 2013, *A&A*, 555, A57
 Geller A. M., Leigh N. W. C., 2015, *ApJL*, 808, L25
 González Hernández J. I., Ruiz-Lapuente P., Tabernero H. M., Montes D., Canal R., Méndez J., Bedin L. R., 2012, *Nature*, 489, 533

- Goodwin S. P., Kroupa P., 2005, *A&A*, 439, 565
- Gough B., 2009, GNU Scientific Library Reference Manual—Third Edition, 3rd edn. Network Theory Ltd.
- Graham M. L., Sand D. J., Zaritsky D., Pritchett C. J., 2015, ArXiv e-prints: 1505.03407
- Hamers A. S., Perets H. B., Antonini F., Portegies Zwart S. F., 2015, *MNRAS*, 449, 4221
- Hamers A. S., Pols O. R., Claeys J. S. W., Nelemans G., 2013, *MNRAS*, 430, 2262
- Harrington R. S., 1972, *Celestial Mechanics*, 6, 322
- Harris W. E., 1996, *AJ*, 112, 1487
- Heggie D., Hut P., 2003, *The Gravitational Million-Body Problem: A Multidisciplinary Approach to Star Cluster Dynamics*
- Heggie D. C., 1975, *MNRAS*, 173, 729
- Heggie D. C., Rasio F. A., 1996, *MNRAS*, 282, 1064
- Heggie D. C., Sweatman W. L., 1991, *MNRAS*, 250, 555
- Hills J. G., 1991, *AJ*, 102, 704
- Hills J. G., Day C. A., 1976, *ApJL*, 17, 87
- Holberg J. B., 2009, *Journal of Physics Conference Series*, 172, 012022
- Holman M., Touma J., Tremaine S., 1997, *Nature*, 386, 254
- Howell D. A., 2011, *Nature Communications*, 2
- Hunter J. D., 2007, *Computing In Science & Engineering*, 9, 90
- Hut P., 1983, *ApJ*, 268, 342
- Hut P., Bahcall J. N., 1983, *ApJ*, 268, 319
- Iben, Jr. I., Tutukov A. V., 1984, *ApJS*, 54, 335
- Innanen K. A., Zheng J. Q., Mikkola S., Valtonen M. J., 1997, *AJ*, 113, 1915
- Ivanova N., 2008, in *Multiple Stars Across the H-R Diagram*, Hubrig S., Petr-Gotzens M., Tokovinin A., eds., p. 101
- Ivanova N., Heinke C. O., Rasio F. A., Belczynski K., Fregeau J. M., 2008, *MNRAS*, 386, 553
- Ivanova N. et al., 2013, *A&AR*, 21, 59
- Kaib N. A., Raymond S. N., 2014, *ApJ*, 782, 60
- Katz B., Dong S., 2011, ArXiv e-prints: 1105.3953
- Katz B., Dong S., 2012, ArXiv e-prints: 1211.4584
- Katz B., Dong S., Malhotra R., 2011, *Physical Review Letters*, 107, 181101
- Kochanek C. S., Adams S. M., Belczynski K., 2014, *MNRAS*, 443, 1319
- Koo J.-R., Lee J. W., Lee B.-C., Kim S.-L., Lee C.-U., Hong K., Lee D.-J., Rey S.-C., 2014, *AJ*, 147, 104
- Kozai Y., 1962, *AJ*, 67, 591
- Kroupa P., 2001, *MNRAS*, 322, 231
- Kushnir D., Katz B., Dong S., Livne E., Fernández R., 2013, *ApJL*, 778, L37
- Kustaanheimo P. E., Stiefel E., 1965, *Perturbation theory of Kepler motion based on spinor regularization. Astronomical observatory*
- Lamers H. J. G. L. M., Gieles M., Bastian N., Baumgardt H., Kharchenko N. V., Portegies Zwart S., 2005, *A&A*, 441, 117
- Leigh N., Geller A. M., 2012, *MNRAS*, 425, 2369
- Leigh N., Sills A., Knigge C., 2011, *MNRAS*, 416, 1410
- Leigh N. W. C., Geller A. M., 2013, *MNRAS*, 432, 2474
- Leigh N. W. C., Geller A. M., 2015, ArXiv e-prints: 1503.07876
- Li G., Adams F. C., 2015, *MNRAS*, 448, 344
- Li G., Naoz S., Kocsis B., Loeb A., 2014, *ApJ*, 785, 116
- Lidov M. L., 1962, *Planet. Space Sci.*, 9, 719
- Lithwick Y., Naoz S., 2011, *ApJ*, 742, 94
- Littlewood J., 1952, *Comm. Sémin. Math. Unvi. Lund [Medd. Lunds Univ. Mat. Sem.]*, Tome Supplémentaire, 143
- Malmberg D., Davies M. B., 2009, *MNRAS*, 394, L26
- Malmberg D., Davies M. B., Hoggie D. C., 2011, *MNRAS*, 411, 859
- Malmberg D., de Angeli F., Davies M. B., Church R. P., Mackey D., Wilkinson M. I., 2007, *MNRAS*, 378, 1207
- Mannucci F., Della Valle M., Panagia N., 2006, *MNRAS*, 370, 773
- Maoz D., Badenes C., 2010, *MNRAS*, 407, 1314
- Maoz D., Badenes C., Bickerton S. J., 2012, *ApJ*, 751, 143
- Maoz D., Mannucci F., 2012, *PASA*, 29, 447
- Maoz D., Mannucci F., Nelemans G., 2014, *ARA&A*, 52, 107
- Mardling R., Aarseth S., 1999, in *NATO ASIC Proc. 522: The Dynamics of Small Bodies in the Solar System, A Major Key to Solar System Studies*, Steves B. A., Roy A. E., eds., p. 385
- Mardling R. A., Aarseth S. J., 2001, *MNRAS*, 321, 398
- Maschberger T., 2013, *MNRAS*, 429, 1725
- Mazeh T., Shaham J., 1979, *A&A*, 77, 145
- McMillan P. J., 2011, *MNRAS*, 414, 2446
- Mikkola S., 1983, *MNRAS*, 203, 1107
- Miller M. C., Hamilton D. P., 2002, *ApJ*, 576, 894
- Milone A. P. et al., 2012, *A&A*, 540, A16
- Moeckel N., Bonnell I. A., 2013, ArXiv e-prints: 1301.6959
- Morais M. H. M., Giuppone C. A., 2012, *MNRAS*, 424, 52
- Naoz S., Fabrycky D. C., 2014, *ApJ*, 793, 137
- Naoz S., Farr W. M., Lithwick Y., Rasio F. A., Teyssandier J., 2011, *Nature*, 473, 187
- Naoz S., Farr W. M., Lithwick Y., Rasio F. A., Teyssandier J., 2013, *MNRAS*, 431, 2155
- Naoz S., Farr W. M., Rasio F. A., 2012, *ApJL*, 754, L36
- Napiwotzki R., 2009, *Journal of Physics Conference Series*, 172, 012004
- Nomoto K., 1982, *ApJ*, 253, 798
- Nomoto K., Iwamoto K., Nakasato N., Thielemann F.-K., Brachwitz F., Tsujimoto T., Kubo Y., Kishimoto N., 1997, *Nuclear Physics A*, 621, 467
- Öpik E., 1924, *Publications of the Tartu Astrofizica Observatory*, 25, 1
- Pejcha O., Antognini J. M., Shappee B. J., Thompson T. A., 2013, *MNRAS*, 435, 943
- Perets H. B., Fabrycky D. C., 2009, *ApJ*, 697, 1048
- Perets H. B., Kratter K. M., 2012, *ApJ*, 760, 99
- Pérez F., Granger B. E., 2007, *Computing in Science and Engineering*, 9, 21
- Perlmutter S. et al., 1999, *ApJ*, 517, 565
- Petrovich C., 2015, ArXiv e-prints: 1506.05464
- Piskunov A. E., Kharchenko N. V., Röser S., Schilbach E., Scholz R.-D., 2006, *A&A*, 445, 545
- Piskunov A. E., Schilbach E., Kharchenko N. V., Röser S., Scholz R.-D., 2007, *A&A*, 468, 151
- Poincaré H., 1892, *Les méthodes nouvelles de la mécanique céleste*, Gauthier-Villars et fils
- Porras A., Christopher M., Allen L., Di Francesco J., Megeath S. T., Myers P. C., 2003, *AJ*, 126, 1916
- Portegies Zwart S., Boekholt T., 2014, *ApJL*, 785, L3
- Prodan S., Murray N., Thompson T. A., 2013, ArXiv e-prints: 1305.2191

- Raghavan D. et al., 2010, ApJS, 190, 1
 Raskin C., Scannapieco E., Rockefeller G., Fryer C., Diehl S., Timmes F. X., 2010, ApJ, 724, 111
 Riess A. G. et al., 1998, AJ, 116, 1009
 Rosswog S., Kasen D., Guillochon J., Ramirez-Ruiz E., 2009, ApJL, 705, L128
 Ruiter A. J., Belczynski K., Fryer C., 2009, ApJ, 699, 2026
 Ruiter A. J., Belczynski K., Sim S. A., Hillebrandt W., Fryer C. L., Fink M., Kromer M., 2011, MNRAS, 417, 408
 Sana H. et al., 2013, A&A, 550, A107
 Sana H. et al., 2014, ApJS, 215, 15
 Saslaw W. C., Valtonen M. J., Aarseth S. J., 1974, ApJ, 190, 253
 Scannapieco E., Bildsten L., 2005, ApJL, 629, L85
 Schaefer B. E., Pagnotta A., 2012, Nature, 481, 164
 Seto N., 2013, Physical Review Letters, 111, 061106
 Shappee B. J., Stanek K. Z., Pogge R. W., Garnavich P. M., 2013, ApJL, 762, L5
 Shappee B. J., Thompson T. A., 2013, ApJ, 766, 64
 Shara M. M., Hurley J. R., 2002, ApJ, 571, 830
 Sigurdsson S., Phinney E. S., 1993, ApJ, 415, 631
 Socrates A., Katz B., Dong S., Tremaine S., 2012, ApJ, 750, 106
 Sumi T. et al., 2011, Nature, 473, 349
 Sundman K. F., 1907, Recherches sur le problème des trois corps. Ex Officina Typographica Societatis Litterariae Fennicae
 Sweatman W. L., 2007, MNRAS, 377, 459
 Tange O., 2011, The USENIX Magazine, 36, 42
 Thompson T. A., 2011, ApJ, 741, 82
 Tokovinin A., 2014, AJ, 147, 87
 Tokovinin A., Thomas S., Sterzik M., Udry S., 2006, A&A, 450, 681
 Tytenda R. et al., 2011, A&A, 528, A114
 Tytenda R., Soker N., 2006, A&A, 451, 223
 Valtonen M., Mikkola S., 1991, ARA&A, 29, 9
 van Kerkwijk M. H., Chang P., Justham S., 2010, ApJL, 722, L157
 Veras D., Raymond S. N., 2012, MNRAS, 421, L117
 Voss R., Nelemans G., 2012, A&A, 539, A77
 Webbink R. F., 1984, ApJ, 277, 355
 Wen L., 2003, ApJ, 598, 419
 Whelan J., Iben, Jr. I., 1973, ApJ, 186, 1007
 Wilson E. B., 1927, Journal of the American Statistical Association, 22, 209
 Wu Y., Murray N., 2003, ApJ, 589, 605
 Wu Y., Murray N. W., Ramsahai J. M., 2007, ApJ, 670, 820
 Zapatero Osorio M. R., Béjar V. J. S., Martín E. L., Rebolo R., Barrado y Navascués D., Bailer-Jones C. A. L., Mundt R., 2000, Science, 290, 103

APPENDIX A: THE COLLISION CROSS SECTION

The dependence of the collision cross section in few-body scattering problems on the incoming velocity and stellar radius has been investigated by a number of studies (e.g., Fregeau et al. 2004; Leigh & Geller 2015), but an analytic

fit to these dependences does not exist in the literature. We present such a fit here in the case of equal mass stars.

Collisions can occur in two different ways: through a three-body interaction or through a two-body interaction. In a three-body interaction the interloping star exchanges momentum with one star of the binary before eventually colliding with the other. In a two-body interaction the interloping star collides into one of the stars of the binary without interacting with the other at all.

For three-body interactions, the collision cross section scales with velocity in the same way that the cross section for exchange does. That is, for $\hat{v} < v_{\text{crit}}$ the velocity scaling is \hat{v}^{-2} and for $\hat{v} > v_{\text{crit}}$ the velocity scaling is \hat{v}^{-6} . The low-velocity scaling is due to gravitational focusing, whereas the high-velocity scaling is likely because the mechanism by which collisions occur in three-body scattering events is similar to the mechanism by which exchanges occur. Exchanges occur when two stars undergo a close approach and exchange momenta (Hut 1983). This ejects one star formerly in the binary and replaces it with the interloping star on a similar orbit. A collision may occur if the momentum exchange places the interloping star on an orbit eccentric enough to lead to a collision. Since the mechanism for collision is similar, we would then expect the collision cross section to display the same \hat{v}^{-6} velocity dependence as the exchange cross section. Note, however, that this is simply a plausibility argument. We do not attempt here to show rigorously that this is the mechanism responsible for the observed velocity dependence. Nevertheless, the numerical calculations indicate that the cross sections indeed show a \hat{v}^{-6} velocity dependence in this regime just like exchange.

We may combine these velocity dependences as we did in Section 4.1 to find the overall cross section:

$$\frac{1}{\hat{\sigma}_{3\text{-body}}} = \frac{\hat{v}^2}{\hat{\sigma}_a} + \frac{\hat{v}^6}{\hat{\sigma}_b}, \quad (\text{A1})$$

where $\hat{\sigma}_a$ and $\hat{\sigma}_b$ are constants of order unity that must be fit to numerical data.

Let us consider now two-body interactions. Like three-body interactions, these exhibit two velocity regimes. However, in this case the two velocity regimes are separated by the escape velocity of the stars, v_{esc} . For $\hat{v} \gg v_{\text{esc}}$, gravitational focusing from the individual stars is negligible and the cross section for collision will approach a constant value equal to the geometric cross section of the stars. For velocities less than v_{esc} , gravitational focusing from individual stars will lead to a \hat{v}^{-2} dependence. For two-body interactions, then, the overall cross section will be

$$\hat{\sigma}_{2\text{-body}} = \hat{\sigma}_{\text{geometric}} + \frac{\hat{\sigma}_c}{\hat{v}^2}, \quad (\text{A2})$$

where the geometric cross section is just given by

$$\hat{\sigma}_{\text{geometric}} = 2\pi \left(\frac{R}{a} \right)^2, \quad (\text{A3})$$

and $\hat{\sigma}_c$ must be fit to numerical data, though it will be of order $\hat{\sigma}_{\text{geometric}} \hat{v}_{\text{esc}}^2$.

The collision cross sections for two- and three-body interactions may then be combined additively to yield the overall collision cross section:

$$\hat{\sigma}_{\text{coll.}} = \hat{\sigma}_{2\text{-body}} + \hat{\sigma}_{3\text{-body}} = \left(\frac{\hat{v}^2}{\hat{\sigma}_a} + \frac{\hat{v}^6}{\hat{\sigma}_b} \right)^{-1} + \frac{\hat{\sigma}_c}{\hat{v}^2} + \hat{\sigma}_{\text{geometric}}. \quad (\text{A4})$$

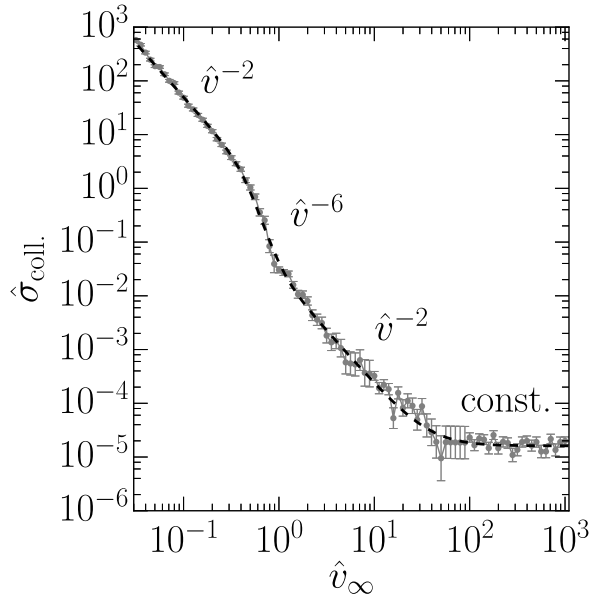


Figure A1. The cross section for a collision to occur in binary-single scattering as a function of the normalized incoming velocity. We show both numerical data (gray points) and a fit to equation (A4) (black dashed line). This system consists of three $1 M_{\odot}$ stars each with a radius of $0.3 R_{\odot}$. The binary orbit is circular with a semi-major axis of 1 AU. The best-fitting parameters are $\hat{\sigma}_a \approx 0.475$, $\hat{\sigma}_b \approx 2.00 \times 10^{-2}$, $\hat{\sigma}_c \approx 2.25 \times 10^{-2}$, and $\hat{\sigma}_{\text{geometric}} \approx 1.61 \times 10^{-5}$.

A fit of equation (A4) to numerical data is shown in Fig. A1. There is an excellent match between the numerical data and the analytic fit.